Archives of Civil and Mechanical Engineering (2024) 24:144
https://doi.org/10.1007/s43452-024-00961-2

ORIGINAL ARTICLE

Low-velocity impact behavior of two-way SFRC slabs strengthened with steel plate

Mohammed Gamal Al-Hagri[1] · M. Sami Döndüren[2] · Tolga Yılmaz[2] · Özgür Anıl[3] · Hakan Erol[4] · Hasan Selim Şengel[4]

Received: 11 November 2023 / Revised: 31 March 2024 / Accepted: 24 April 2024

Abstract
Structural systems and structural elements can often suffer severe damage or even completely collapse under the effect of sudden dynamic impact loading, which is a different type of loading that is not considered during their design. Research on how structures behave under impact loading and how they can be strengthened to perform better against this type of loading has increased to avoid such undesirable severe damage. Within the scope of this study, it is aimed to improve the behavior and increase the performance of two-way steel fiber-reinforced concrete (SFRC) slabs, one of the leading structural elements that can be affected by impact loading, using steel fiber concrete (SFC) and placing steel plates on the surface of the RC slab. Within the scope of the study, the effects of placing FRC as layers in different positions within the slab and placing the steel plate on different surfaces of the slabs were examined. Impact loading was applied using a drop weight test setup designed by the authors, and the acceleration–time, displacement–time, and impact loading–time behaviors of the RC slabs were measured and interpreted. The use of fiber concrete in RC slabs and strengthened with steel plates increased the maximum acceleration values by an average of 3% and 113%, respectively. The use of fiber concrete in RC slabs reduced the maximum displacement and residual displacement values by an average of 2% and 25%, respectively. Placing steel plates on the slabs reduced the maximum displacement and residual displacement values by an average of 270% and 199%, respectively. In addition, the energy absorption capacities of RC slabs were calculated, and how they were affected by experimental variables was examined. Numerical analyses of the RC slabs tested in the study were also conducted using ABAQUS finite element software, and the results obtained were compared with the experimental ones.

Keywords RC slab · Impact load · Strengthening · Steel fiber · Steel plate · FEA

1 Introduction

Structures can be exposed to impact loading due to many different reasons. RC slabs are at the forefront of the structural elements affected by impact loading. The causes of impact loading can be counted as the collision of vehicles on a bridge plates, explosions occurring outside or inside structural systems, RC shear walls built outside the structures to protect them from explosions, the collision of objects coming from rockfall, landslide, avalanche, flood or wind effects on RC slabs or shear walls in structural systems. Even during the gradual demolition works of structures with explosive effect, it is possible to apply impact loading to the RC slabs by falling off the RC bearing elements destroyed due to the explosion. The behavior of RC slabs under the effect of such loads is an important subject that needs to be investigated. During their design, structural elements or whole systems, including RC slabs, are designed under the influence of static loads and dynamic loads, such as earthquakes and winds, but not designed for a special type of loading, such as sudden dynamic impact loading, which has a very high intensity although its duration is extremely short. For this reason, it is a frequently

✉ Özgür Anıl
oanil@gazi.edu.tr

[1] Department of Civil Engineering, Istanbul Aydın University, Istanbul, Turkey

[2] Civil Engineering, Konya Technical University, Konya, Turkey

[3] Department of Civil Engineering, Gazi University, Ankara, Turkey

[4] Civil Engineering Department, Eskişehir Osmangazi University, Eskişehir, Turkey

Published online: 08 May 2024

encountered problem that structural elements are severely damaged or completely collapsed under the effects of sudden dynamic impact loading. It aims to investigate RC slabs' behavior under the impact loads to avoid unwanted damages and collapse mechanisms, which are at the forefront of structural elements that can often be exposed to impact loading in structures, as stated in the examples above. When the literature is explored, it is seen that there are studies examining the behavior of RC slabs under the effect of sudden dynamic impact loading. In these studies, researchers investigated the effects of variables that may influence the behavior of RC slabs subjected to impact loadings, including the condition of support [1], opening in the slabs [2], and the ratio of reinforcement [3].

In the literature, it is possible to come across many studies examining strengthening methods to improve the behavior of reinforced concrete structural elements under the influence of static loads and increase their performance. Studies in which it is strengthened with high strength RC corbel with FRP [4] and Self-Compacted Reinforced Concrete Corbel with FRP [5] have been found in the literature. However, there are much more limited studies in the literature examining strengthening methods developed to improve the behavior of reinforced concrete elements under impact loading. It was observed from the results of the conducted studies that RC slabs can be severely damaged and may even collapse under the effect of sudden dynamic impact loading. For this reason, research on various strengthening methods to improve the behavior of RC slabs under the effect of sudden dynamic impact loads and to increase their performance levels has increased. In addition to the studies on the strengthening of RC slabs with composite FRP [6] and TRM strips [7], studies on the strengthening of RC slabs with fiber-reinforced concrete [8] and steel plates [9] are also found in the literature. When these studies are examined, it is seen that various types of fibers are used to improve the behavior of RC slabs and other RC elements under impact loading. The effects of the hybrid use of more than one fiber simultaneously have been investigated. In the studies, the effect of changes that can be made in concrete mixtures and the effect of additive materials other than fibers on improving the impact behavior of RC structural elements were also investigated, and the optimum fiber ratio and effective fiber types were tried to be determined. When the literature is examined, it is seen that there are many more studies examining the behavior of fiber-reinforced concrete under the influence of static loading, but the number of studies under the effect of impact loading is more limited. Studies have appeared in the literature in which reinforced concrete precast hybrid deep beams [10] were examined under static loads, and high-performance reinforced arched-hybrid self-compacting concrete deep beams [11] were tested under the effect of static loads.

It is observed in the literature that there are studies on improving the performance of RC slabs under impact loading using different types of composite materials, fiber-reinforced concrete, and steel elements. However, it is thought that the developed strengthening details require special workmanship, use high-cost composite materials, have long application times, and contain complex details that make applying these strengthening methods difficult. Based on this idea, it aims to develop a strengthening method that can increase the performance level of RC slabs that are easy to apply, not costly, does not require special labor during application, and do not contain very sensitive details. As a result of the comprehensive literature review made for this purpose, an experimental study was planned to experimentally investigate the use of steel fiber-reinforced concrete and steel plates to improve the impact performance of RC slabs. A comparison between these two methods was made and interpreted. Steel fiber-reinforced concrete and steel plates have been preferred because they are cheaper, easier to apply, fast, and do not require special labor compared to other strengthening methods. The variables examined within the scope of the study were chosen as the use of steel plate and steel fiber-reinforced concrete layer on different surfaces of RC slabs. Sudden dynamic impact loading was applied to RC slabs using a free drop weight test setup designed by the authors, and an impact energy of 2.9224 kJoules was applied at a constant energy level by dropping the 198.6 kg impactor from a height of 1.5 m. The acceleration–time, displacement–time, and impact loading–time histories were measured under the impact load applied to the RC slab specimens, and then, using these values, impact load–displacement graphs were drawn for the specimens, and the amount of energy absorbed by the RC slabs was calculated. By interpreting all the measured and calculated values, the effect of steel fiber-reinforced concrete layer and steel plate techniques used for the strengthening of RC slabs on their behavior was examined. In the second part of the study, numerical analyses of RC slabs were carried out using ABAQUS finite element software. By comparison with the experimental results, it was investigated to what extent the finite element model could give consistent and realistic results compared to the experimental ones.

2 Experimental study

2.1 Test specimens and materials

$1000 \times 1000 \times 120$ mm two-way RC slab specimens were produced and tested under constant energy impact loading. The same reinforcement ratio was used in all the RC slab test elements. Deformed reinforcement with 8 mm diameter and 100 mm intervals was placed in both directions on both

tensile and compressive surfaces. All test elements' geometric dimensions and reinforcement details are identical, given in Fig. 1. RC slabs are strengthened with two techniques to improve their behavior and performance under the applied constant energy level impact loading. The strengthening methods chosen to be examined within the scope of the study were determined as the use of steel fiber-reinforced concrete layer and steel plate layer on different surfaces of the RC slabs. Details of the strengthening methods used in the RC slab test elements are presented in Fig. 2.

Moreover, the properties of the RC slabs considered in the experimental program are presented in Table 1. The Specimen-1 reference specimen was produced from non-fibrous normal concrete without strengthening in the test series. Specimen-2 in the experimental program is a specimen whose concrete was produced by adding 1.0% by volume steel fiber. In Specimen-3, 4, 5, and 6 included in the experimental program, fiber-reinforced concrete layer having a height of 40 mm (1/3 of the height of the RC slab) and produced by adding 1.0% by volume steel fiber was used on different slab surfaces. The 40 mm high fiber-reinforced concrete layer was placed in four different positions in Specimen-3, 4, 5, and 6, only on the lower face, only on the upper face, only on the middle layer, and on both the lower and upper surfaces of the RC slab, respectively (Fig. 2). Specimen-7, Specimen-8, and Specimen-9 were strengthened using a 1.0 mm thick steel plate and produced from 1.0% by volume steel fiber-reinforced concrete. Two different types of concrete mixtures were used to produce the specimens.

The only difference between the concretes used in the experimental study is that steel fiber with a volume fraction of 1.0% was added to the second concrete mixture. Five standard cube concrete samples of 150 × 150 mm were taken from each mixture to determine the compressive strength of the concretes used in the study. The concrete compressive strengths of the cube samples were determined by storing them in the same curing conditions as the RC slab and testing them at the time of the experiments. The average compressive strengths of normal concrete and steel fiber-reinforced concrete used in the study were 44.4 MPa

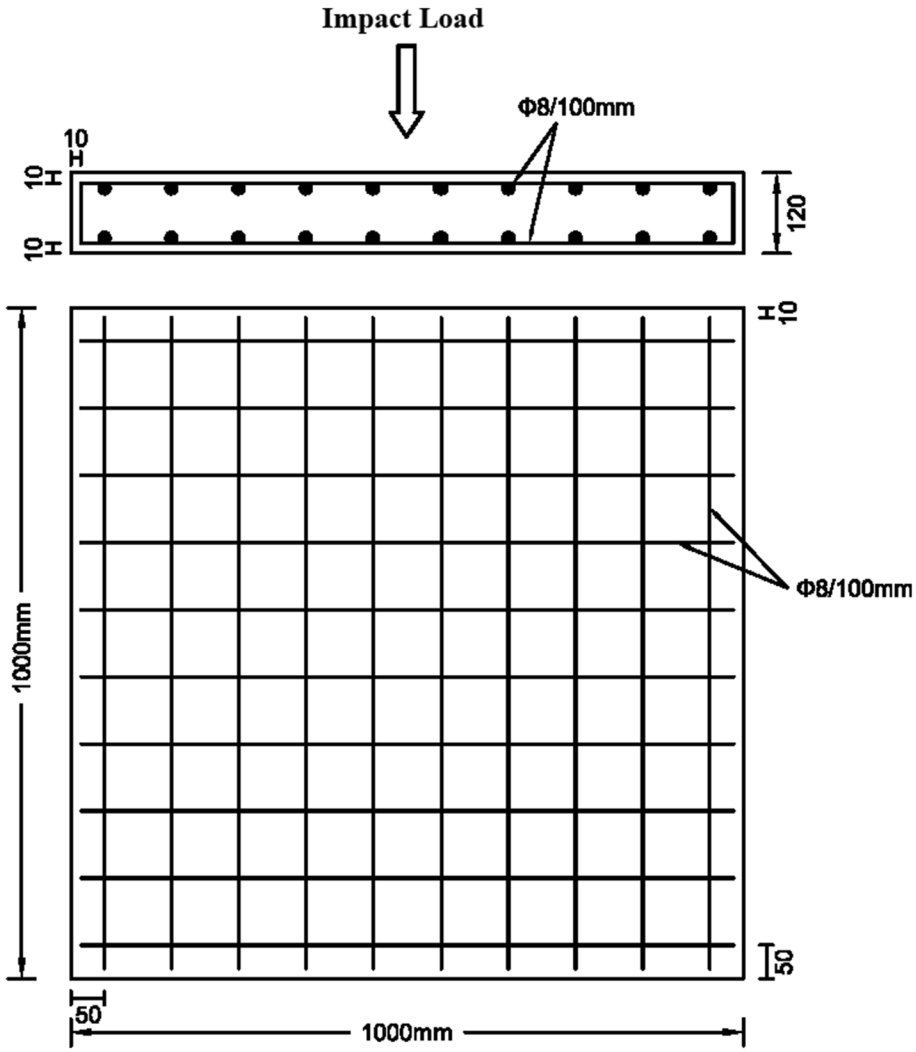

Fig. 1 Dimensions and reinforcement details of specimens (dimensions are mm)

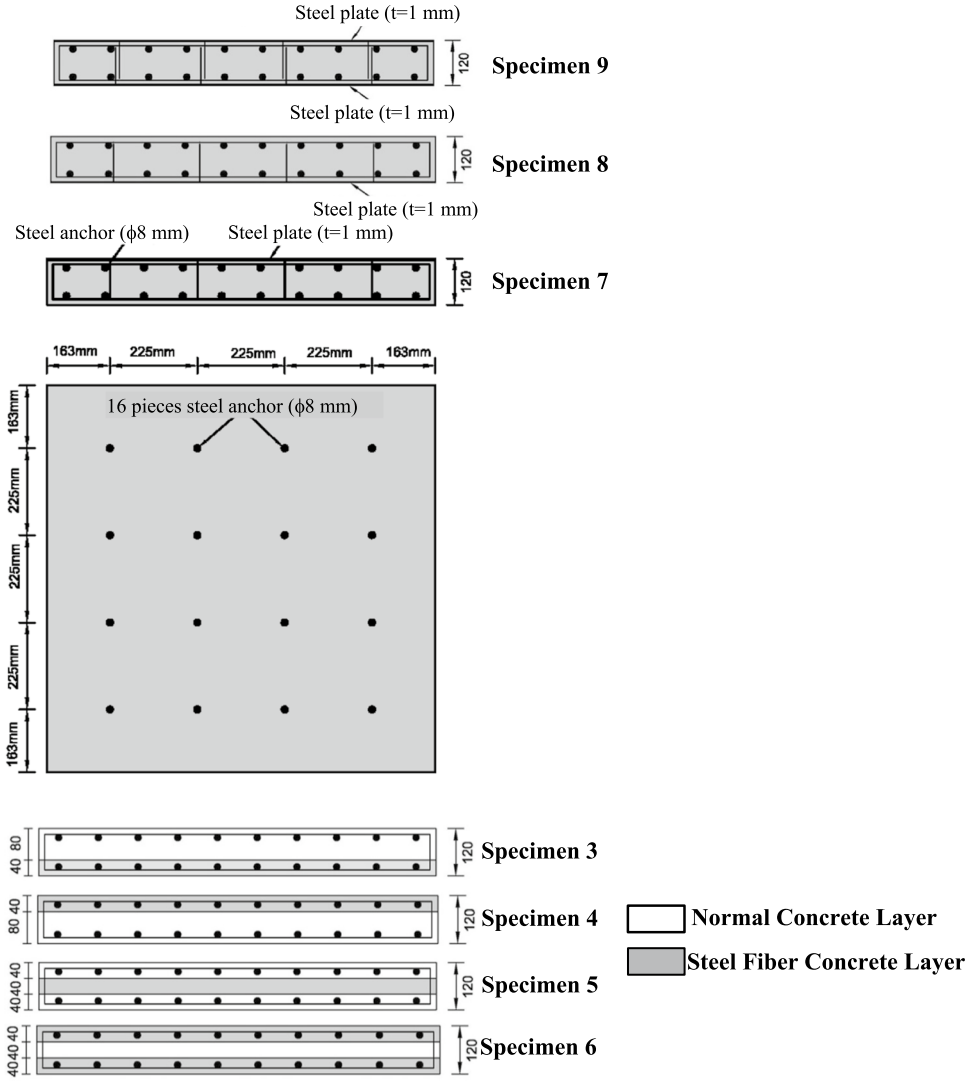

Fig. 2 Strengthening details of specimens (dimensions are mm)

Table 1 Properties of specimens

Spec. no.	Compressive strength of concrete f_c (MPa)	Remarks
1	44.4	Normal strength concrete without steel fiber (reference)
2	48.5	1.0% steel fiber-reinforced concrete by volume
3	44.4/48.5	One-third of the floor height, the top layer of 1.0% steel fiber-reinforced concrete
4	44.4/48.5	One-third of the floor height, the bottom layer of 1.0% steel fiber-reinforced concrete
5	44.4/48.5	1.0% steel fiber-reinforced concrete in the middle layer, one-third of the floor height
6	44.4/48.5	1.0% steel fiber-reinforced concrete with top and bottom layers one-third of the floor height
7	48.5	1.0% by volume steel fiber-reinforced concrete with 1 mm steel plate on the upper surface
8	48.5	1.0% by volume steel fiber-reinforced concrete with 1 mm steel plate on the bottom surface
9	48.5	1.0% by volume steel fiber-reinforced concrete with 1 mm steel plate on the upper and bottom surfaces

and 48.5 MPa, respectively. All the compressive strengths obtained from the five cube samples taken to determine the concrete compressive strengths are very close to each other, and the standard deviation and variation values were calculated to be very small. Concrete cube samples were tested with a computer-controlled hydraulic press with an adjustable loading speed (0.9 MPa/s). To determine the tensile strength of the concrete types used in the specimens,

two different tests were carried out: the cylinder splitting test and the flexural tensile test. Tests were carried out at a speed of 0.05 MPa/s on five 150 × 300 mm standard cylinder samples taken from the concrete mixture used to produce each specimen. The splitting tensile strengths of the without fiber and fiber-added concretes used to produce the specimens were determined as 1.99 MPa and 3.75 MPa, respectively. The flexural tensile strengths of the concrete mixtures used in the production of the specimens were determined by applying a four-point bending test to standard samples of 50 × 75 × 360 mm dimensions. The average flexural tensile strength values of without fiber and fiber concrete types were determined as 5.04 MPa and 10.75 MPa, respectively. The material mixture quantities used in the production of concrete without steel fiber and fiber used in the experimental study are given in Table 2.

The properties and geometric details of the 50 mm long hooked-end steel fibers used in the production of the fiber-reinforced concrete used in the study are given in Table 3. An axial tensile test was applied to three samples to determine the mechanical properties of the 8 mm diameter deformed reinforcement used in the production of specimens. The mechanical properties obtained from the tests are very close to each other, and the standard deviation and variation values are very low. The reinforcement's average yield strength, tensile strength, and elastic modulus values were calculated as $f_{sy} = 491.73$ MPa, $f_{su} = 597.22$ MPa, and E = 204 GPa, respectively. Axial tensile tests were conducted with a computer-controlled test setup with adjustable speed (0.1 mm/s). To determine the mechanical properties of the St37 class 1.0 mm thick steel plate used for the strengthening in Specimen-7, 8, and 9 test elements, three standard axial tensile specimens taken from the material of the plate in the form of three wish-bones were tested in the same way. The average yield strength, tensile strength, and elastic modulus values obtained from the tests were calculated as $f_{sy} = 266$ MPa, $f_{su} = 381$ MPa, and E = 199 GPa, respectively. Photographs taken from the production stages of the specimens are presented in Fig. 3. After the concrete casting was completed, the specimens were removed from the mold within 2 days. For 19 days, curing was applied by covering them with wetted burlap and plastic tarpaulin to slow the evaporation, and for the last 7 days, they were left to dry in the laboratory. Both fiber-reinforced concrete layer and steel plate strengthening techniques selected to improve the performance of the specimens under impact loading were applied during production while pouring the concrete of the specimens. Sixteen anchor rods having a diameter of 8 mm, the positions of which are given in Fig. 2, were welded to the steel plate, and the steel plate was placed on the RC slab immediately after the concrete pouring was completed to increase the adherence of the 1.0 mm thick steel plate with the RC slab test elements.

Table 2 Concrete mixture design for 1 m^3

Concrete type	Cement (kg)	Water (kg)	Aggregate (kg)		Superplasticizer (0.8%) (kg)	Steel fiber (1%) (kg)
			Fine	Coarse		
Without fiber	350	189.85	953.86	774.99	2.8	–
With fiber	350	189.85	953.86	774.99	2.8	78.5

Table 3 Properties of steel fiber

Properties	Value
Appearance	Bright, steel wire
Type	Cold drawing
Edge geometry	Corrugated
Edge angle	45°
Length	50 mm
Diameter	1.0 mm
Slenderness ratio	50
Tension strength	1200 MPa

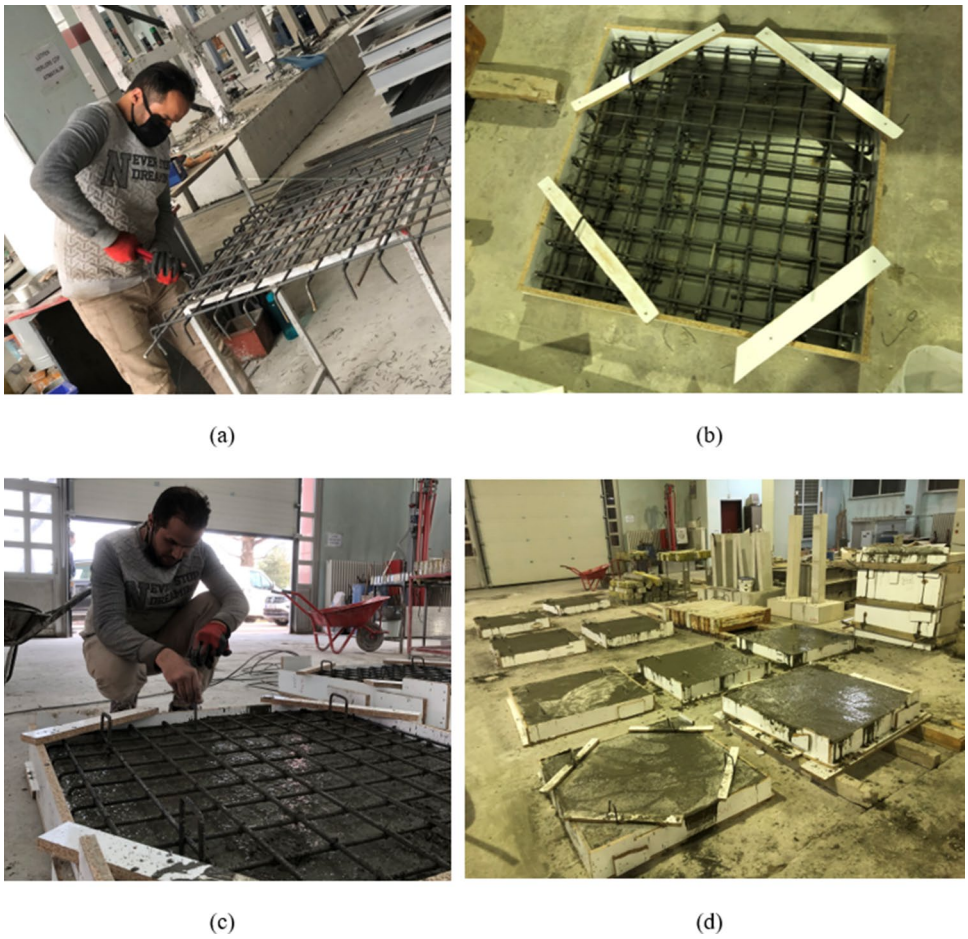

Fig. 3 Manufacturing stages of RC slabs, **a** preparation of reinforcement, **b** prepared formwork and reinforcement, **c** layer height control in the hybrid slab, **d** specimens ready for testing

2.2 Test setup and instrumentations

Impact loading on the specimens was applied using a free drop weight test setup designed by the authors, which was previously used in many studies in the literature [2]. The details of the experiment and measurement setup used in the experimental study are presented in Fig. 4. A constant energy impact load of 2.9224 kJoule was applied to the RC slabs by dropping a 198.6 kg impactor from a height of 1.5 m. The dimensions of the RC slabs tested in the experimental study were determined by taking into account the capacity of the free weight test setup used for the tests and the measurement capacities of the sensors used in the measurements. In the test setup used in the experimental study, tests can be carried out by dropping a weight of 250 kg from a maximum height of 1.5 m. In the tests carried out, a weight of 200 kg, close to the maximum capacity, was dropped from 1.5 m. The geometric dimensions of the tested RC slabs were also selected according to the impact loading energy magnitude that can be applied in the test setup. A reasonable size of specimen has been determined that can sustain damage at a level that can be monitored at the energy level of the applied impact loading and where the differences caused by the variables examined in the experimental study can be monitored. In addition, the geometry of the experimental specimens was determined by taking into account the sensitivities and capacities of the measurement sensors used in the experimental study. The dimensions of the steel support system used were determined according to the geometric dimensions of the RC slabs tested in the experimental study, and the support system was produced using high-strength ST52 class structural steel.

Impact loading on the RC slabs was applied and measured by a dynamic load cell placed between two plates made of high-strength steel with dimensions of $150 \times 150 \times 20$ mm, placed exactly at their midpoints. By placing the dynamic load cell between two steel plates, it was both protected and the applied load was applied to all specimens from the same point and distributed to an identical area, thus preventing any possible eccentricity during impact loading. Details about the positions of the steel plates with a dynamic load cell placed on the specimens and the locations of other acceleration and displacement sensors according to the position of these plates are given in Fig. 4. An impactor head made of high-strength steel with hemispherical geometry was used to apply the

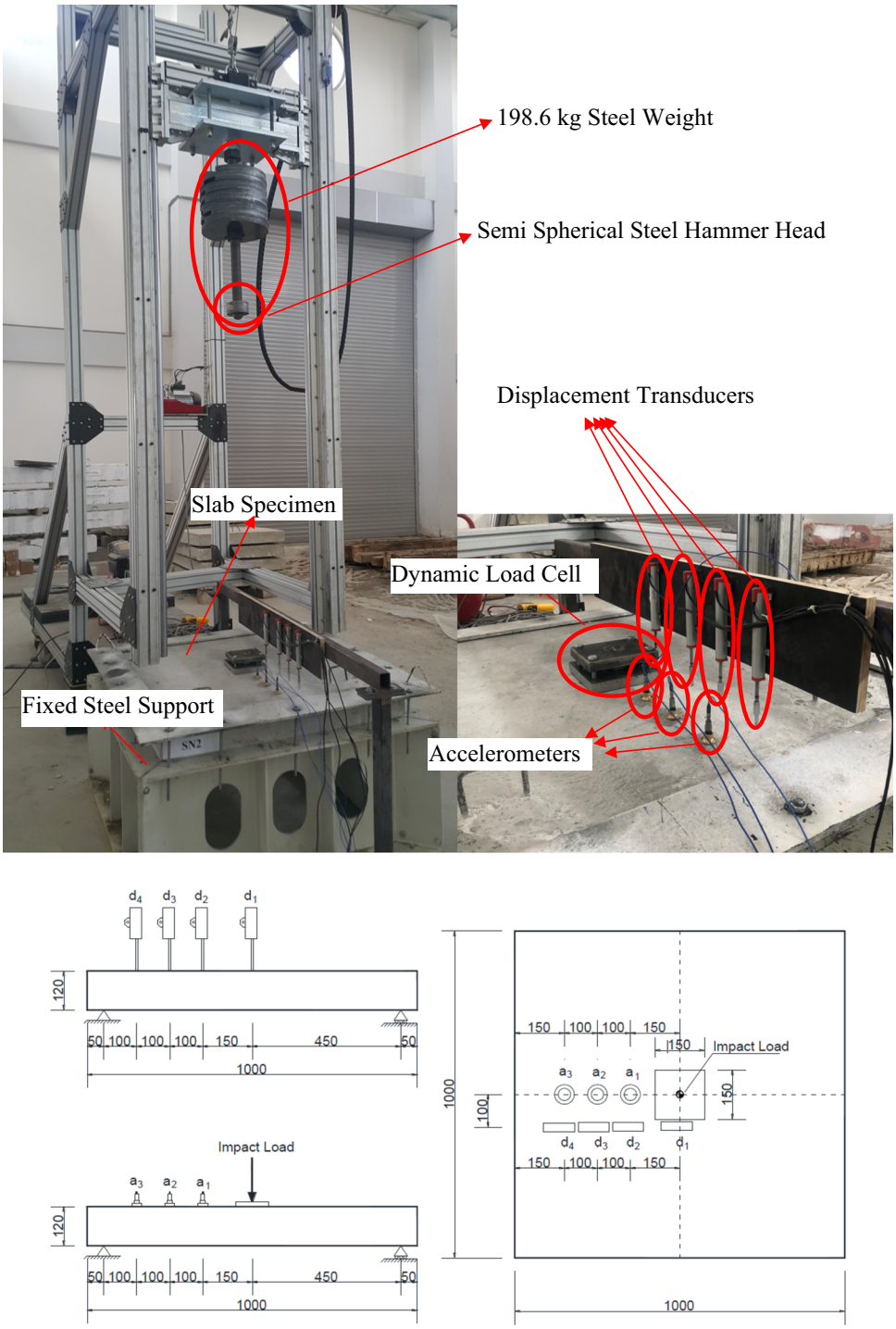

Fig. 4 Test setup and instrumentations

constant energy impact load to the specimens. The acceleration–time, displacement–time, and impact loading–time histories that occurred due to the application of impact load to the specimens were measured and interpreted. By measuring the acceleration from three points and the displacement from four points from each of the specimens, it is aimed to investigate how the displacement and acceleration happened in the RC slabs due to the application of the impact load are distributed and how their changes occur as we move away from the impact point. Reinforced concrete slabs were placed on a support setup made of steel profiles and supported on all four sides to be accepted as fixed support. The 50 mm long sections of the RC slabs are placed on the support setup produced from steel profiles in both directions and by tightening the steel plates placed on it with bolts and preventing the horizontal and vertical

movements along with rotations, it is supported in such a way that it can be accepted as fixed support.

In addition, the energy absorption capacities of the specimens were calculated. The amount of energy absorbed by the RC slabs was calculated using the impulse-momentum theorem. According to the impulse-momentum theorem, the impulse equals the change in momentum (ΔM) [12]. Change in momentum at the moment of impact was calculated using Eq. 1. Impulse (I_p) was obtained by calculating the area under the impact load–time graph. The rebound velocity (V_r) was calculated using Eq. 2 using the impulse value. The energy absorbed by the sample (E_{ab}) was calculated by subtracting the impact energy (E_{Impact}) from the rebound energy using Eq. 3 [13].

$$\Delta M = m \times \left(V_{\text{Impact}} - V_{\text{r}}\right) = I_{\text{P}} \tag{1}$$

$$V_{\text{r}} = V_{\text{Impact}} - \frac{I_{\text{P}}}{m} \tag{2}$$

$$E_{\text{ab}} = E_{\text{Impact}} - -0.5 \times m \times V_{\text{r}}^2 \tag{3}$$

where ΔM is the change in momentum, m is the weight of the hammer (198.6 kg), V_{Impact} is the velocity of the hammer at impact (4.4 m/s), V_r is the rebound velocity of the hammer after impact, I_p is the impulse, E_{ab} is the energy absorbed by the sample, and E_{Impact} is the applied impact energy (2922.4 J).

3 Experimental results and discussion

Acceleration–time, displacement–time, and impact load–time histories were measured due to the impact load applied to the RC slab specimens. The results obtained were interpreted, and the effects of the strengthening methods applied in the study and the experimental variables on the behavior of the slabs under the impact load were investigated. Among the three acceleration measurements measured from the specimens, the maximum acceleration–time values measured from the closest accelerometer to the point where the impact load is applied (a_1 accelerometer, 150 mm distance from the impact point) are presented in Fig. 5. Among the four displacement–time measurements taken from the specimens, d_1 maximum displacement–time graphs measured on the slab symmetry axis

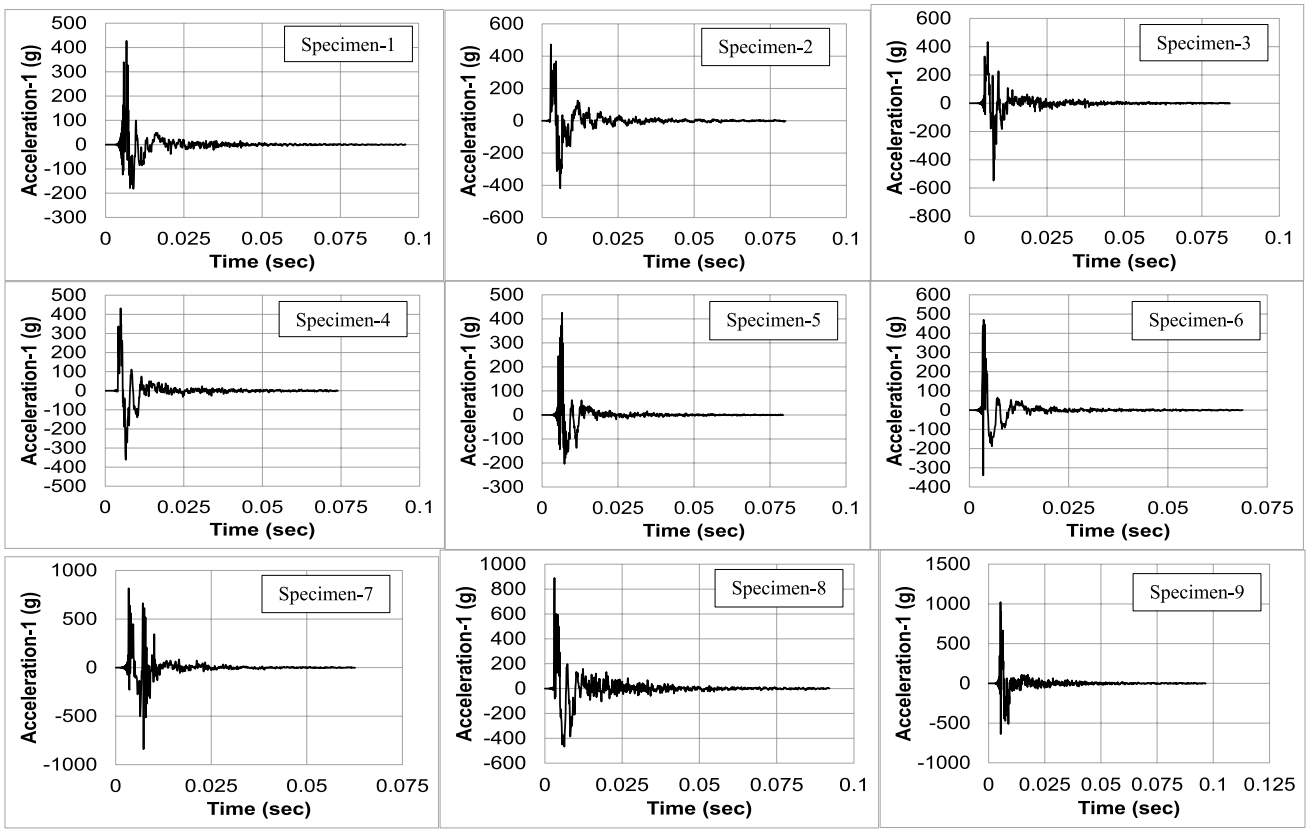

Fig. 5 Maximum acceleration–time graphs of specimens

from a distance less than 100 mm from the point where the impact load is applied are given in Fig. 6. The impact load–time graphs applied to the specimens are given in Fig. 7, and the impact load–displacement graphs created by combining the maximum displacement–time and impact load–time graphs measured from the specimens with the same time interval are given in Fig. 8. The photographs showing the crack distribution and damage conditions on the tensile surfaces of the RC slabs after being subjected to the impact load are presented in Fig. 9. The results obtained from the tests of the specimens are given in Table 4. Table 4 gives the maximum and minimum acceleration values of the maximum acceleration–time graph closest to the impact point among the three acceleration measurements measured from each specimen. Similarly, the maximum and residual displacement values obtained from the maximum displacement–time graph measured from the closest point to the impact point among the four displacement–time measurements measured from the RC slabs are presented in Table 4. The maximum displacement value is calculated by summing the absolute value of the maximum and minimum displacement values of the displacement–time graph, in which the maximum displacement behavior is measured. The maximum displacement value measured from the RC slabs was calculated by adding the maximum downward and upward displacements of the RC slab to the absolute value using the graph of the sensor where the maximum displacement was measured. It is the absolute maximum value of the deformation occurring in the RC slab. The residual displacement value is obtained from the maximum displacement–time graph as the permanent plastic deformation value remaining on the RC slab after the vibration motion caused by the impact load is damped. When the maximum impact load values given in Table 4 are examined, it is seen that they are quite close to each other for all the RC slab specimens. This is expected since the impact energy level applied to the specimens is the same. This result shows that the energy loss that may occur from friction in the free drop weight test setup used in the experiments is negligible, and the device is suitable for impact tests. The differences observed in the maximum impact load values are due to the differences in the stiffness and strength of the tested RC slabs [6]. RC slabs between Specimen-1 and Specimen-6 have approximately the same maximum impact load values, averaging 45.16 kN. This result shows that the strengths and stiffnesses of the first six specimens between Specimen-1 and Specimen-6 are quite close. The

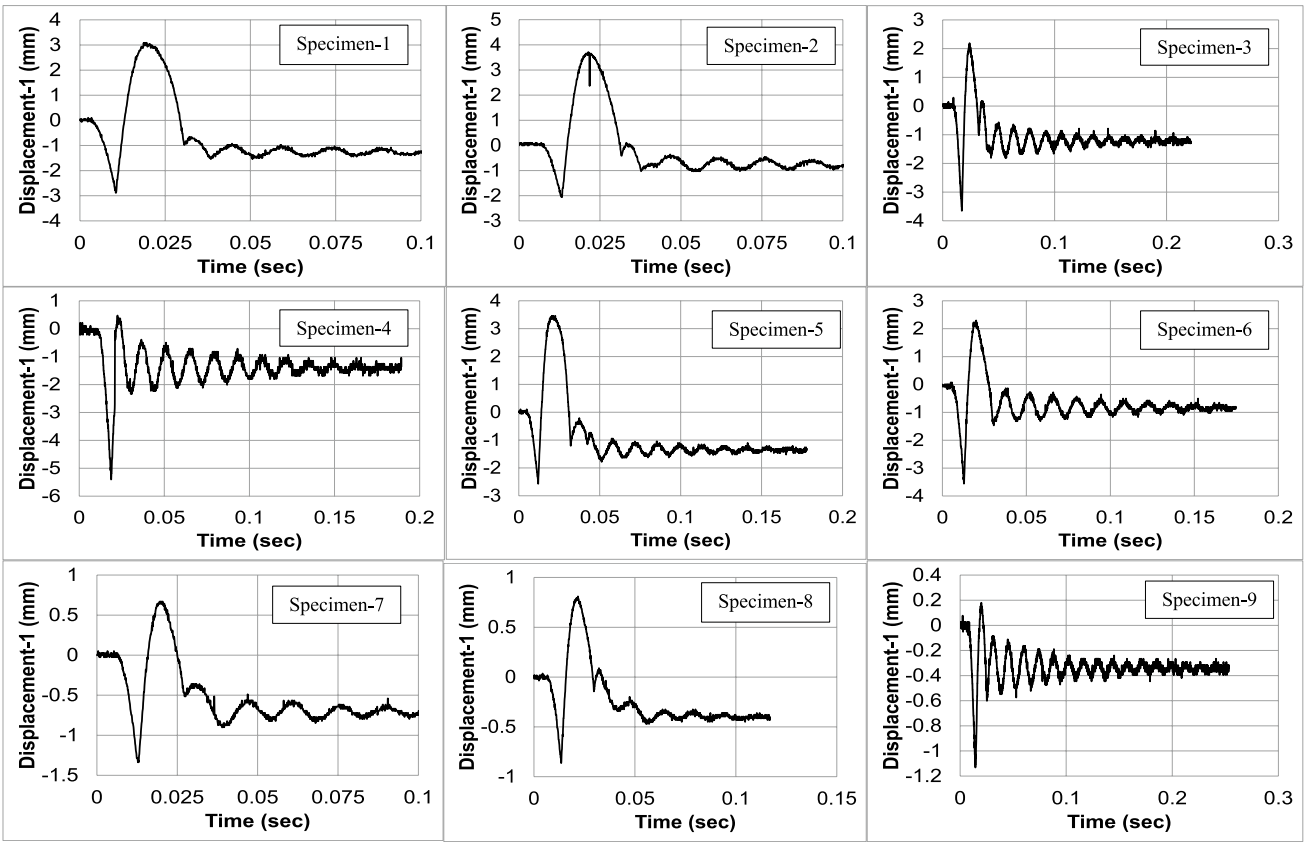

Fig. 6 Maximum displacement–time graphs of specimens

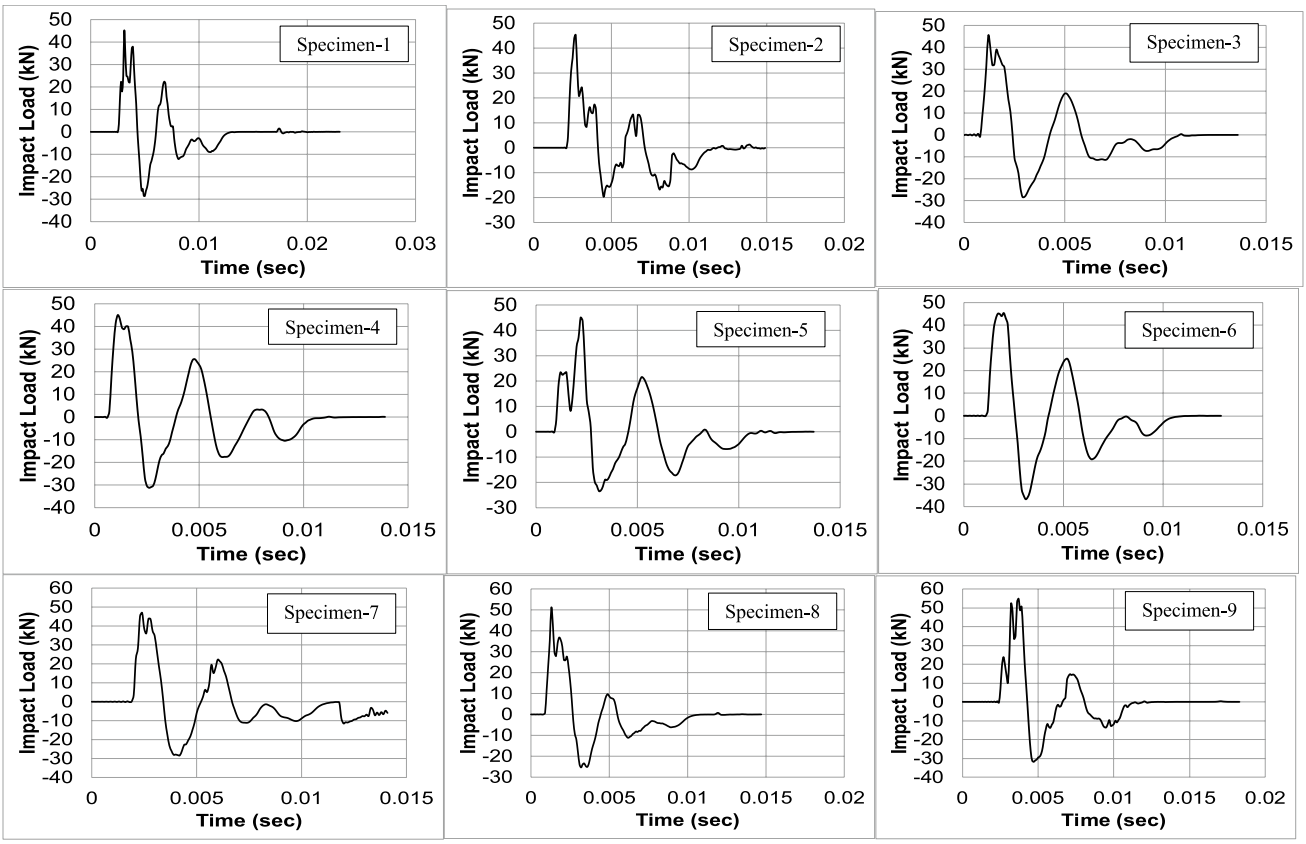

Fig. 7 Impact load–time graphs of specimens

fact that the maximum impact load values of the first six specimens are very close to each other is thought to be due to the close compressive strengths of the concretes used in the production of the slabs. It is observed that the impact load increased in Specimen-7, 8, and 9 specimens, in which steel plates were used for strengthening. This shows that using steel plates significantly increases the rigidity and strength of the RC slab. It is observed that the increase in stiffness and strength is greater when the steel plate is used on the tensile surface of the RC plate. Maximum impact load value of Specimen-8, which was used steel plate on tensile surface, was 13.5% higher than the non-strengthened reference Specimen-1. Among all the RC slabs tested within the scope of the study, the highest maximum impact load value was 54.97 kN and was obtained in Specimen-9, which was strengthened with steel plates on its lower and upper surfaces. The maximum impact load measured from Specimen-9 is 22.1% greater than that of the non-strengthened reference Specimen-1. When the results obtained in terms of basic mechanics principles are examined, considering that the weight dropped with a constant weight and from a fixed height has a constant energy level, it is seen that the main reason for the change in the loading applied at the point of impact is the toughness, rigidity, and strength of the specimen to which the loading is applied. Since the SFRC slabs strengthened with steel plate have much higher toughness, rigidity, and strength than the slabs using SFC in different layers without steel plate, the maximum impact loading values measured were calculated to be 13% higher on average in the specimens without steel plate.

When the experimental results are examined, it is observed that the use of steel fiber-reinforced concrete layer and steel plate layer in RC slabs increases the maximum acceleration values. It is observed that the increase ratio in the maximum acceleration values is much higher when the steel plate layer is used. Using a steel fiber-reinforced concrete layer with a volume fraction of 1.0% by volume in the Specimen-2 increased the maximum acceleration value by 10.6% compared to the non-fibrous normal concrete Specimen-1. The increase in the maximum acceleration value is thought to be because steel fiber added to the concrete mix increases the RC slab's strength, rigidity, and toughness. This result is in parallel with some other studies found in the literature [14]. It is thought that steel fiber added to the concrete of specimens causes the acceleration waves that occur because of the impact load to reach the accelerometers more quickly without being damped by increasing the

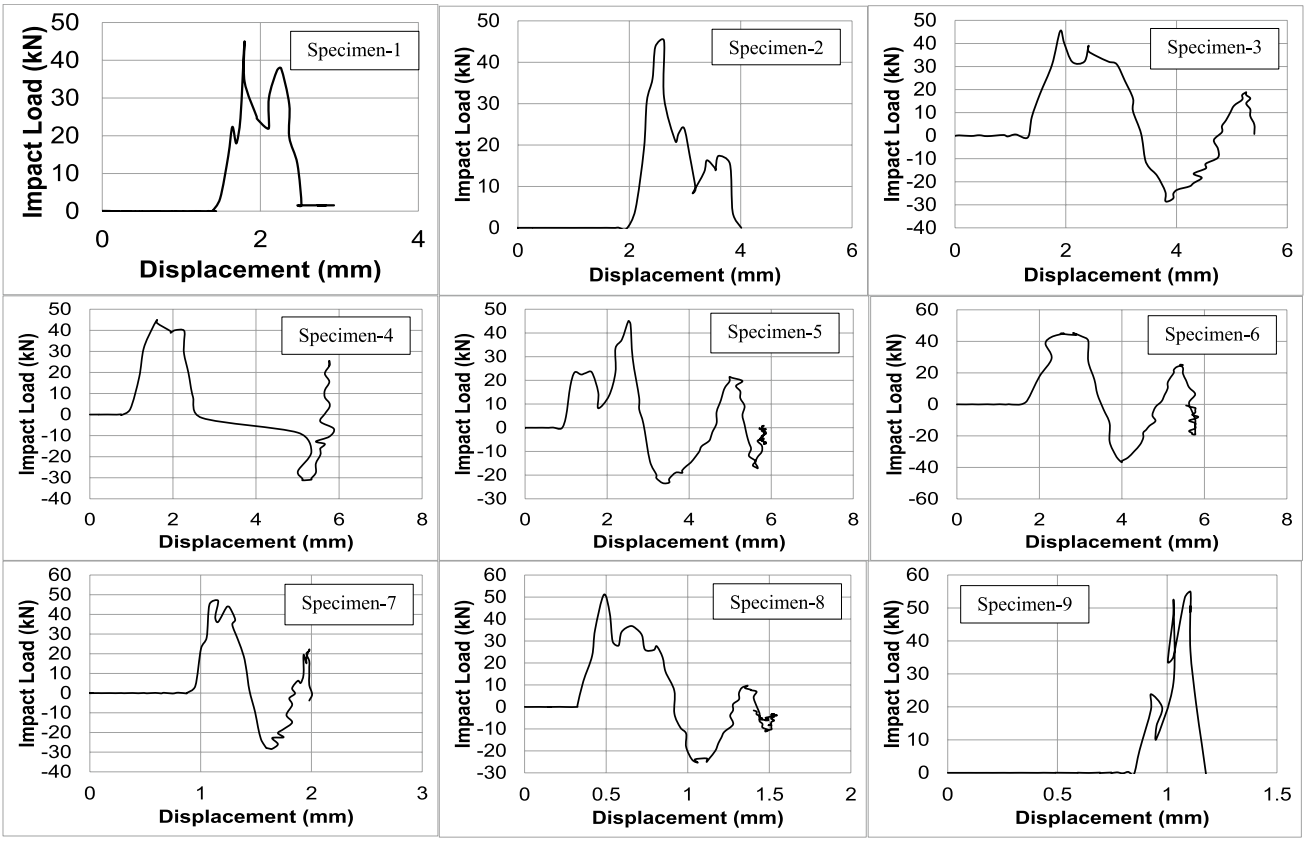

Fig. 8 Impact load–displacement graphs of specimens

rigidity and toughness of the RC slabs [3]. It is thought that adding steel fiber to the concrete mix increases the toughness and stiffness of the concrete and improves the performance of the RC slab under impact load.

The maximum acceleration values measured from Specimen-3, 4, and 5, in which a steel fiber-reinforced concrete layer was used as 1/3 of the RC slab thickness, were obtained very close to the maximum acceleration value of reference Specimen-1 produced with non-fibrous concrete. The maximum difference between the maximum acceleration values measured from Specimen-3, 4, and 5 and the maximum acceleration value of reference Specimen-1 was calculated as 1.5%. This result shows that the use of steel fiber-reinforced concrete layer as only a single layer in the RC slabs was not able to sufficiently increase the slab's overall rigidity, strength, and toughness. However, the maximum acceleration value of Specimen-6, in which fiber-reinforced concrete with a volume fraction of 1.0% was used on upper and lower surfaces, increased by 10% compared to the reference Specimen-1 produced with normal concrete. The increasing percentage in the maximum acceleration value of Specimen-6 was very close to that of Specimen-2, produced entirely from 1.0% steel fiber-reinforced concrete. The use of steel fiber in concrete in the production of RC slabs has not only had an effect on the compressive strength of concrete, but also has a much more positive effect on the tensile strength of concrete. There was only a 9% increase in the compressive strength of the steel fiber concrete with the addition of 1.0%. However, the tensile strength values obtained from the cylinder splitting test of the added 1.0% steel fiber concrete increased by 88% and the tensile strength values obtained from the flexural tensile strength tests increased by 113%. It is thought that under the effect of impact loading, a tensile stress field is formed on the lower tensile surface of the RC slabs and in the front part of the impact point where the impactor contacts, and the increase in the tensile strength of the specimens is the main effective parameter in improving the performance under the effect of impact loading.

The second strengthening technique examined within the scope of the study is the use of 1.0 mm thick steel plates in the RC slabs at different positions. The additional use of steel plates in the specimens produced using 1.0% by volume steel fiber-reinforced concrete significantly increases the maximum acceleration values and improves the overall performance of the RC slabs under impact loading. It is determined that improvement in the performance of RC slabs depends on the number and location of the steel plates used for strengthening. The maximum acceleration values

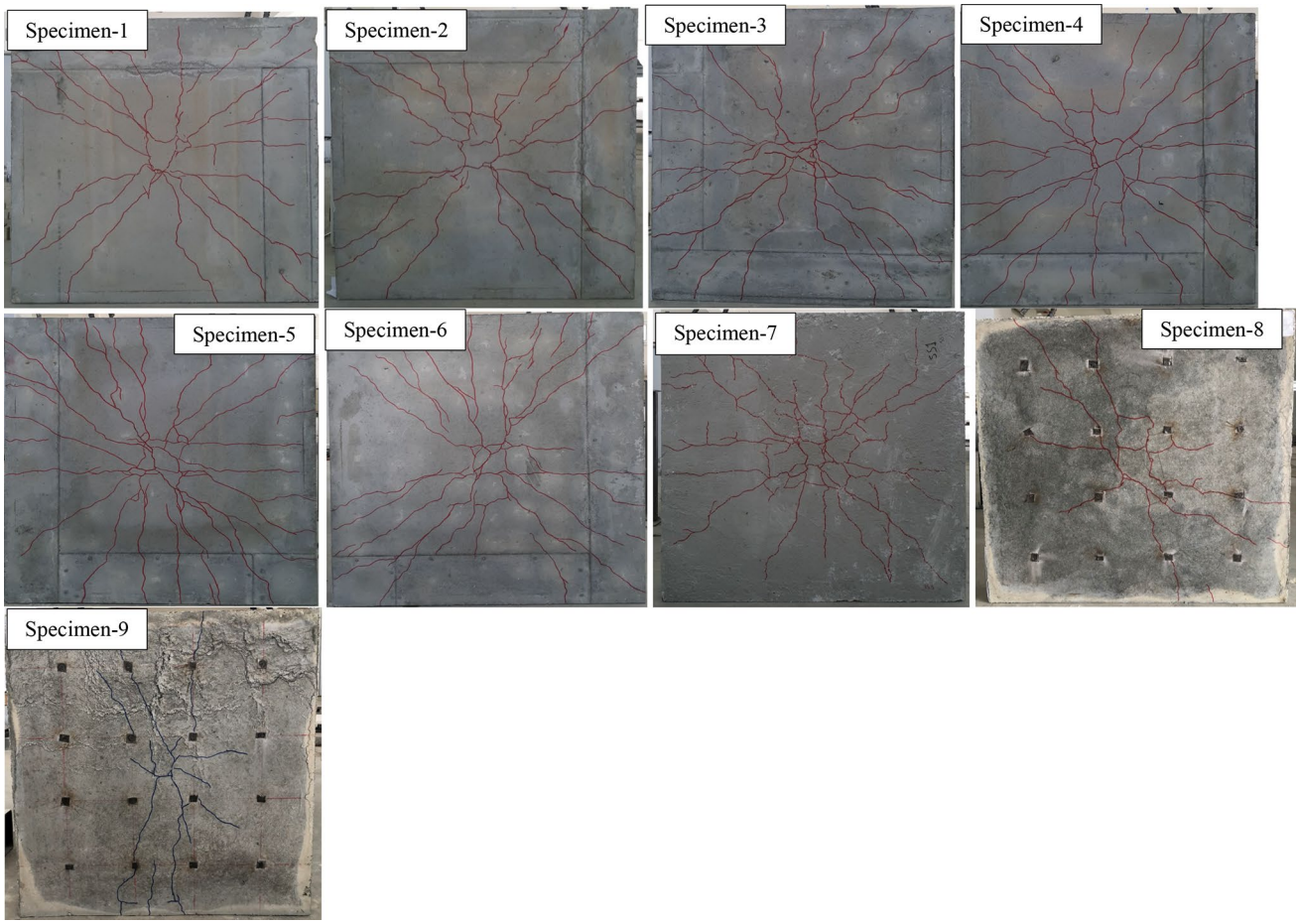

Fig. 9 Crack distribution of specimens after test

measured from Specimen-7, which has a steel plate on its upper surface where the impact load is applied, are 91.2% and 72.9% higher than Specimen-1 and Specimen-2, respectively. The maximum acceleration value of Specimen-8, in which the steel plate is placed on the tensile surface, is higher than that of Specimen-1 and Specimen-2 by 108.1% and 88.2%, respectively. It is thought that the increased percentages of the acceleration obtained in the Specimen-8 are greater than in Specimen-7 because the use of steel plate on the tensile surface of the slab results in a higher increase in toughness, rigidity, and flexural strength. The highest increase in the maximum acceleration occurred in Specimen-9, in which a steel plate was used on both the compressive and tensile surfaces. The maximum acceleration of Specimen-9 is 139.3% and 116.4% greater than that of Specimen-1 and Specimen-2, respectively. It is thought that using steel plates on both surfaces of the RC slab increases flexural strength, stiffness, and toughness at much higher rates, resulting in higher performance under impact load [15]. Steel plates added to the reinforced concrete slab test elements were effective against the tensile stress field occurring at the point where the impactor contacts with the effect of impact loading and the tensile stresses occurring on the lower surface of the slabs due to the bending deformation effect. It is thought that steel plates cause slabs to deform much less, absorb more energy, and cause less damage.

Table 4 Experimental results

Spec. #	Maximum acceleration (g)		Displacement (mm)		Impact load (kN)
	Maximum	Minimum	Maximum	Residual	
1	427.33	−181.99	5.97	1.29	45.02
2	472.46	−418.76	5.76	0.77	45.20
3	433.64	−547.10	5.84	1.29	45.35
4	431.46	−361.28	5.87	1.31	45.01
5	425.41	−203.66	6.03	1.31	45.04
6	470.12	−339.48	5.85	0.80	45.34
7	816.85	−839.53	2.01	0.72	46.98
8	889.27	−467.00	1.67	0.41	51.08
9	1022.59	−637.75	1.31	0.32	54.97

It is observed that, in general, use of 1.0% by volume steel fiber in the production of RC slabs has a positive effect on the maximum and residual displacement values and causes a reduction in them both. It was found that the maximum and residual displacement values are similarly affected by the variables examined within the scope of the study and showed a parallel behavior trend. The maximum displacement value of Specimen-2, produced using 1.0% volume steel fiber, is 3.6% lower than that of the reference Specimen-1, produced using normal concrete. Steel fiber caused a higher reduction in the residual displacement value. The residual displacement value of Specimen-1 is 67.5% greater than Specimen-2. It is thought that the decrease in the maximum and residual displacement values using steel fibers is because they obstruct the propagation and growth of cracks and increase the rigidity and toughness of the RC slab. The residual plastic displacement value of the RC slab produced with steel fiber-reinforced concrete being much lower than that produced from normal concrete is thought to be because steel fiber concrete exhibits better strain hardening behavior than normal concrete. As a result of material tests, it was determined that the addition of steel fiber to reinforced concrete slabs significantly increased the flexural tensile and cylinder splitting tensile strengths. The fibers added to the concrete prevented the formation of fewer, wider cracks and compensated for the fracture energy transferred to the slabs due to impact loading by creating many more and thinner micro cracks. This mechanism has resulted in an increase in the number of cracks and a decrease in their width, a decrease in the maximum displacement in the slabs, and a much greater decrease in the residual plastic displacement value, especially after the vibration caused by impact loading is damped. Maximum displacement values of Specimen-3, 4, 5, and 6, in which steel fiber-reinforced concrete layer was used in 1/3 of the thickness of the RC slab (40 mm), showed values close to that of reference Specimen-1. Although the decrease percentage in the maximum displacement value is higher in Specimen-4 and Specimen-6, where the steel fiber-reinforced concrete layer is used on the tensile slab surface, the values are generally close. The maximum residual displacement values of Specimen-3, 4, and 5, which have a single steel fiber-reinforced concrete layer, are close to each other and similar to that of the reference Specimen-1. The maximum residual displacement value of Specimen-1 is 61% greater than the Specimen-6, in which two steel fiber-reinforced concrete layers were used.

It is observed that using steel plate layers along with steel fiber in RC slabs significantly reduces the maximum and residual displacement values. The maximum displacement and plastic residual displacement values of the reference Specimen-1 are 197% and 79.2% greater than the Specimen-7, which uses a steel plate on the upper surface where compressive stress occurs, respectively. The maximum displacement and plastic residual displacement values of the reference Specimen-2 are 186.6% and 6.9% greater than the Specimen-7, which uses a steel plate on the upper surface where compressive stress occurs, respectively. The maximum displacement and plastic residual displacement values of the reference Specimen-1 are 257.5% and 214.6% greater than the Specimen-8, which uses a steel plate on the bottom surface where tension stress occurs, respectively. The maximum displacement and plastic residual displacement values of the reference Specimen-2 are 244.9% and 87.8% greater than the Specimen-8, which uses a steel plate on the bottom surface where tension stress occurs, respectively. The maximum displacement and plastic residual displacement values of the reference Specimen-1 are 355.7% and 303.1% greater than the Specimen-9, which uses a steel plate both of the upper and bottom surfaces, respectively. The maximum displacement and plastic residual displacement values of the reference Specimen-2 are 339.7% and 140.6% greater than the Specimen-9, which uses a steel plate both of the upper and bottom surfaces, respectively. The significant decrease in the maximum and plastic residual displacement values of Specimen-7, 8, and 9, in which the steel plate was used, is thought to be due to the remarkable increase in the flexural strength, stiffness, and toughness values of the RC plates due to the use of steel plate. Concrete is a building material with very low flexural tensile strength and axial tensile strength and is described as brittle. In order for the sudden dynamic impact effects caused by an explosion or the ballistic effects of a remotely fired ammunition on the concrete to be absorbed by the concrete and form an anti-ballistic shield, it is necessary to reduce the brittleness of the concrete to very low levels compared to conventional concrete and increase the tensile strength to a large extent. Because, as seen in Fig. 10, the type of stress that causes damage in collisions is tensile stress. When evaluated in terms of continuum mechanics, an area where tensile stress is concentrated in a certain region (seen in red in Fig. 10) occurs at the contact point of two objects colliding with each other. This resulting tensile stress field progresses inwards perpendicularly from the point where the impact occurred within the target continuous environment over time. In the strengthening technique proposed within the scope of the study, it is aimed to carry this intense tensile stress concentrated area, which occurs with 1.0 mm thick steel plates, by steel, which has a much higher capacity in terms of tensile stress, instead of concrete. The results obtained from the experimental study showed that the strengthening technique developed using steel plates was successful in significantly reducing the maximum displacement and residual displacement values and increasing the performance of the slabs under impact loading.

When the crack distribution formed after the application of the impact load to the RC slabs was examined, it was

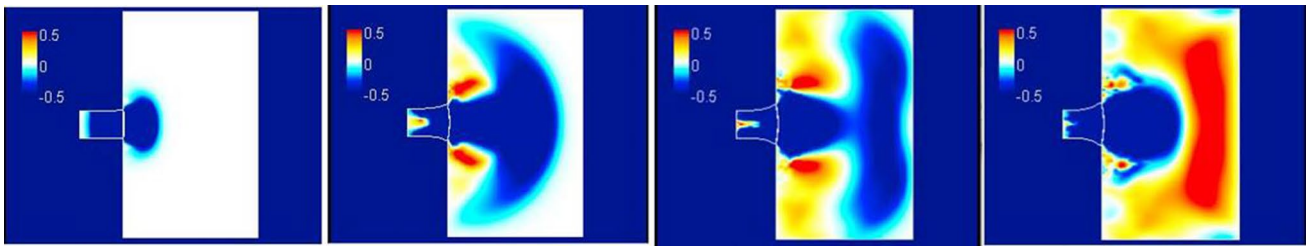

Fig. 10 Stress fields formed in two impacting objects

observed that most of the cracks occurred on the tensile surface of the specimens and in the middle region of the slab where the impact load was applied (Fig. 9). No visible crack was detected on the compressive surface of the specimens on which the impact load was applied. In addition, although crack distribution is concentrated on the specimens' tensile surface, no concrete cover scabbing occurred on this surface. It was observed that the widths of the cracks concentrated in the middle region of the tensile surface were wider in the middle region of the slab where the load was applied, and the width of the cracks decreased as they moved away from this region. It was observed that the cracks on the tensile surface of the RC slabs developed diagonally starting from the midpoint of the slab toward the corner points and that circular radial cracks occurred exactly around the application point of the impact load. It was observed that the crack width decreased with the use of steel fiber in RC slabs. Using steel fiber in the concrete mixture limited the increase in crack widths under impact loading, similar to the effect of static loading. It provided the slab with multiple cracking behaviors, in which many capillary cracks with a much smaller width are formed instead of a smaller number of wider cracks [16]. This cracking behavior was observed in the specimens with a fiber-reinforced concrete layer on their tensile surface. Fewer cracks with much bigger widths were observed in the specimens produced from normal concrete. Using a steel plate layer and steel fiber in the RC slabs significantly limited the damage by reducing the number and width of cracks to a great extent. Using the steel plate layer on the tensile surface of the RC slabs further reduced the damage level and limited the cracks compared to using it on the compressive surface. Using steel plates on the tensile surface of the RC slab significantly increased the specimen' flexural strength, rigidity, toughness, and cracking resistance. As a result, the number and width of cracks decreased significantly in the specimens with steel layers. As stated above, adding steel fiber to increase the tensile stress capacity of the concrete to limit the cracks, that occur as a result of the stress accumulation in the area where the tensile stress occurring within the slab is concentrated with the energy transferred from the impactor to the reinforced concrete slab due to the impact loading, has been partially successful in reducing and distributing the widths of the cracks. However, placing a steel plate with a much higher tensile strength in the area where the tensile stress of the slab is concentrated showed a much more successful result.

During the tests, the acceleration–time histories were measured from three different points. Interpretations about how the acceleration happened in the RC slabs due to the impact loading effect distributed and changed on the slab were made using these measurements. Graphs showing the variation of the maximum values of the acceleration–time distributions on the specimens concerning the distance from the point where the impact load is applied are presented in Fig. 11. When the graphs given in Fig. 11 are examined, it can be seen that the maximum acceleration values in the RC slabs without the steel plate layer decreased linearly as they moved away from the symmetry axis. On the other hand, in the RC slabs with a steel plate layer, the variation of acceleration values concerning the distance from the symmetry axis shows a change that a 2nd-degree parabolic curve can define. When the graphs presented in Fig. 11 are examined, it is seen that in the specimens with a steel plate layer, the maximum acceleration values and damping decrease occur much faster as they move far from where the impact load is applied. Steel plates added to RC slabs have increased the toughness, rigidity, and strength of the slabs to a much greater extent. It can also be seen from the results presented

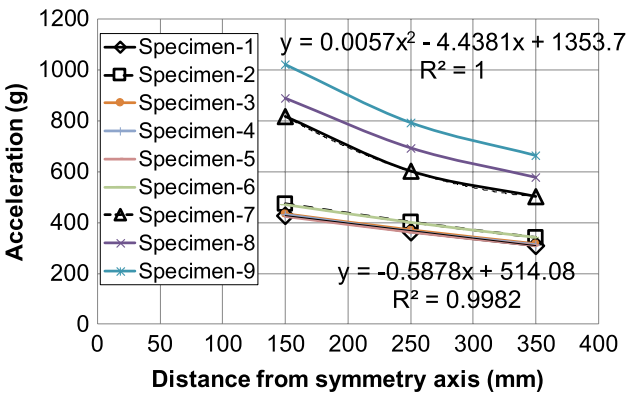

Fig. 11 Variation of accelerations measured from specimens with distance

Table 5 Calculation of energy dissipated by specimens

Spec. #	E_{Impact} (Joule)	V_{Impact} (m/s)	I_p (kN-s)	V_r (m/s)	E_{ab} (Joule)
1	2922.40	4.4	1492.62	3.12	1958.43
2	2922.40	4.4	1441.78	2.86	2110.33
3	2922.40	4.4	1486.76	3.09	1976.59
4	2922.40	4.4	1467.42	2.99	2035.35
5	2922.40	4.4	1491.49	3.11	1961.96
6	2922.40	4.4	1451.68	2.91	2081.78
7	2922.40	4.4	1322.13	2.26	2416.45
8	2922.40	4.4	1245.16	1.87	2575.28
9	2922.40	4.4	1194.23	1.61	2663.96

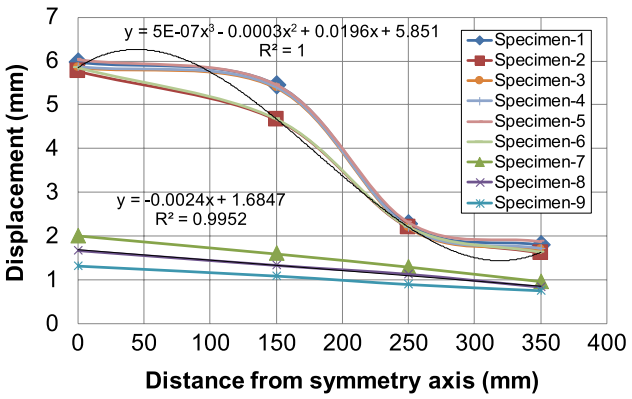

Fig. 12 Variation of displacements measured from specimens with distance

in Table 5 that the amount of energy absorbed by RC slabs increased significantly as a result of the addition of steel plates. The amount of energy absorbed by the specimens strengthened by adding steel plates was calculated to be 26% higher on average than the slabs produced using only FRC. These results are important reasons explaining why acceleration values decrease more rapidly in steel plate slabs as they move away from the midpoint of the slab where impact loading is applied.

On the other hand, in the specimens with a steel fiber-reinforced concrete layer, the rate and speed of the decrease in the acceleration values remain much lower as they move away from the point where the impact load is applied. The displacement–time distributions were measured from four points in total, starting exactly from the symmetry axis of the specimens. The variation of the maximum displacement values of the RC slabs concerning the distance from the symmetry axis is presented in Fig. 12. When Fig. 12 is examined, it is seen that the variation of the maximum displacement values concerning the distance from the symmetry axis in the RC slabs with no steel plate layer can be defined with a cubic function. In the RC slabs with a steel plate layer, the variation of the maximum displacement values concerning the distance from the impact point is linear. When the functions and the changes of the maximum displacement values given in Fig. 12 are examined, it is seen that the maximum displacement values of the specimens with a steel fiber-reinforced concrete layer decrease more rapidly as they move away from the point where the impact load is applied. Still, much larger displacements occurred than in the specimens with a steel plate layer. Much fewer displacement values were measured in the specimens with a steel plate layer, and these values show a slower decreasing trend as they move away from the symmetry axis. When Fig. 12 is examined, it is seen that the maximum displacement distribution resulting from the impact loading in the specimens produced using only SFRC is concentrated in a limited region near the midpoint of the slab where the impact loading is applied and the deformation cannot spread to the entire slab. However, it can be seen that in the slabs strengthened using steel plate, the deformation caused by impact loading is distributed more effectively by the steel plate to the entire slab and remains at a much more limited level.

The energy absorbed by the RC slabs was calculated using the impulse-momentum theorem, and the results are presented in Table 5. While calculating the impact energy, the energy loss due to air resistance and friction in the test device was neglected. In addition, while calculating the energy absorbed by the specimens, the energy absorbed by the support and the energy losses due to noise and heat were neglected [13]. When the impactor used in the impact load application hits the specimen, the RC plate absorbs some of the impact energy through deformation and cracking, and the rebound of the impactor dissipates the rest of the energy. Considering these assumptions, the energies dissipated by the RC slabs in Table 5 have been calculated. When the energy absorption capacity values of the RC slabs given in Table 5 are examined, it is observed that the energy absorption capacities of the specimens between Specimen-2 and Specimen-6, which were produced using only steel fiber-reinforced concrete, are on average 3.8% higher than Specimen-1 reference specimen.

On the other hand, the energy absorption capacities of the specimens between Specimen-7 and Specimen-9, in which the steel plate layer was used in addition to fiber-reinforced concrete, are, on average, 30.3% higher than the Specimen-1 reference specimen. Adding a steel plate layer to the RC slabs is observed to give much more successful results regarding energy absorption capacity than using only a steel fiber-reinforced concrete layer. Although the specimens with a steel plate layer had much less displacement and fewer cracks with smaller widths, they showed much more energy absorption capacity than those with steel fiber-reinforced concrete layers. Considering this result, it is thought that adding a steel layer increases the flexural strength, stiffness,

and toughness of the RC slabs while effectively limiting the displacement values. The fact that the specimens having a steel plate layer absorbed much more energy with much less deformation shows that specimens strengthened with this method can carry a load with much higher impact energy and that their impact performance is much higher.

4 Numerical analysis

In the numerical study, 3D finite element models of the RC slabs tested within the scope of the study were generated using ABAQUS software. ABAQUS is a simulation program capable of modeling the behavior of elements of various materials subjected to different types of loads. Since the specimens were tested under impact loading, this study solved the finite element models using ABAQUS/Explicit solver. An explicit solver was specifically designed to solve efficiently discontinuous nonlinear dynamic problems such as impact and blast [17]. An explicit solver can perform incremental dynamic analysis and provides various material models. The results of the finite element analysis performed using ABAQUS software were evaluated and compared with the experimental results of the RC slabs.

The finite element models of the RC slabs tested within the scope of the experimental study were modeled to have exactly the same geometric dimensions, support conditions, applied strengthening details, and load application form as in the experimental study. As an example, the finite element model generated for Specimen-1 is presented in Fig. 13. Eight-node solid elements with reduced integration (C3D8R) were used in modeling the concrete slab. The

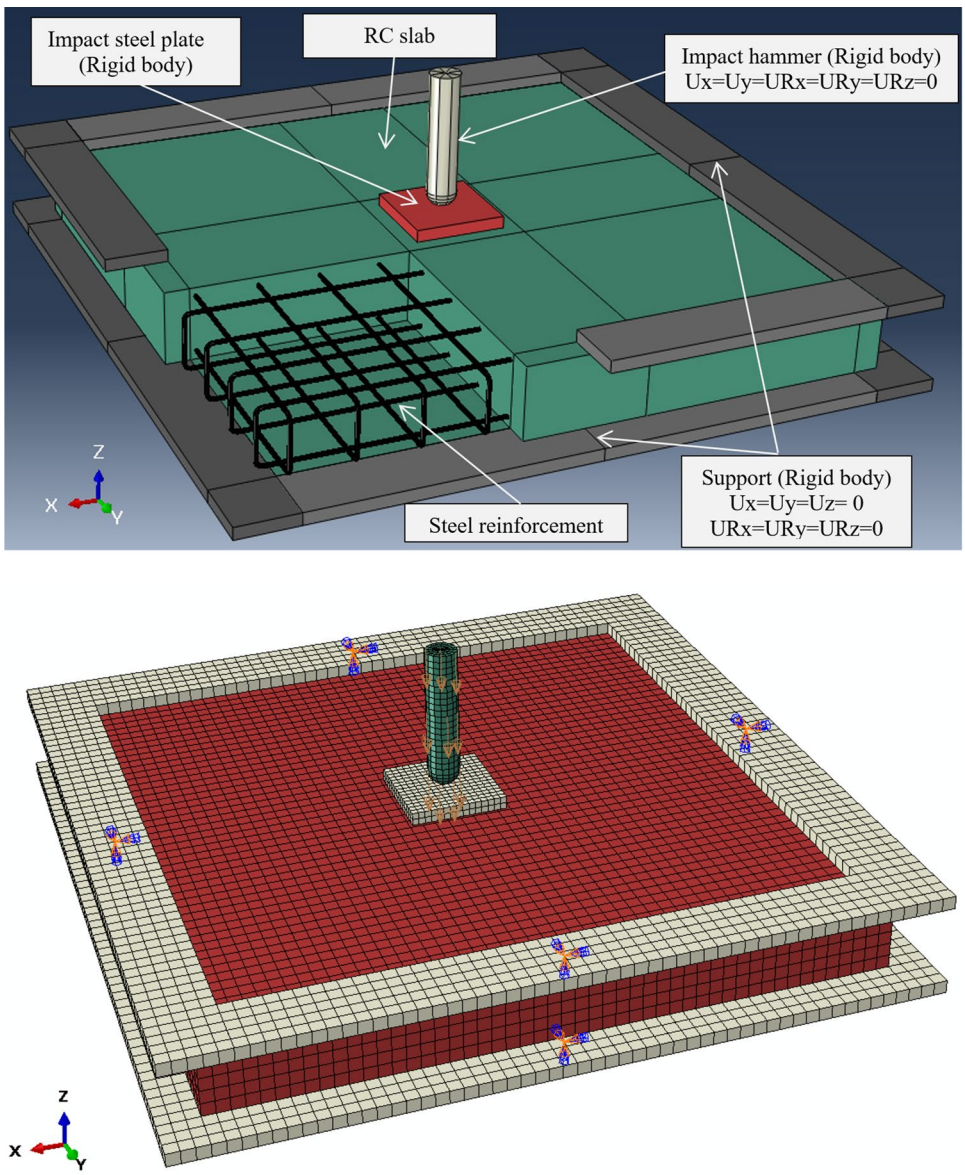

Fig. 13 Finite element model and mesh of Specimen-1

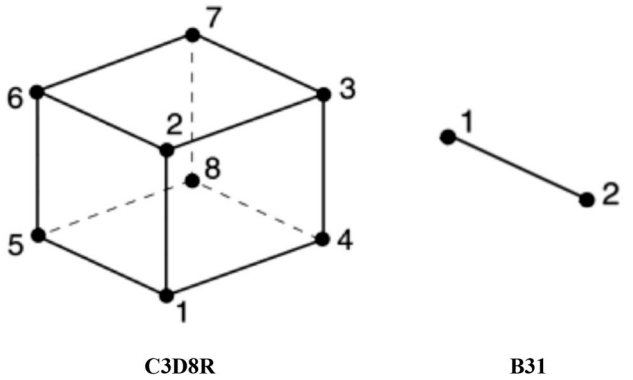

Fig. 14 Element types used in the finite element model

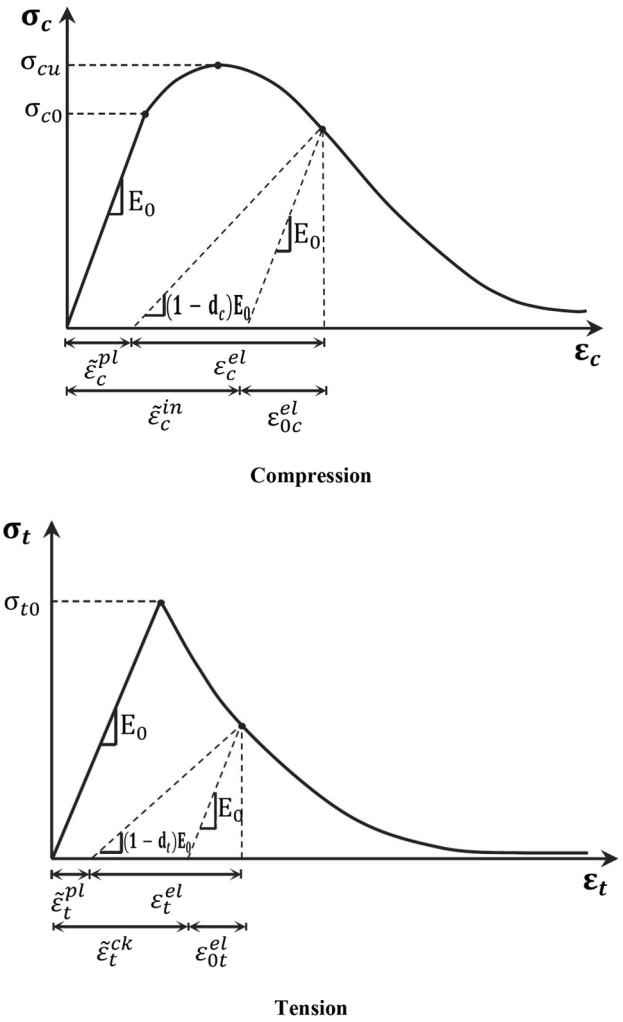

Fig. 15 Constitutive material models of concrete damage plasticity (CDP) concrete material model in compression and tensile

hourglass viscose option was used to stop the formation of zero energy modes [18]. The steel reinforcement was modeled using the two-node beam element B31. The mechanical behavior of steel reinforcement was defined using the classical metal plasticity model. The embedded region constraint defined the interaction between steel reinforcement and concrete. C3D8R and B31 elements used in finite element models are shown in Fig. 14. These two elements are the preferred and used elements in the modeling of concrete and steel reinforcement in reinforced concrete elements subjected to impact loads [19]. The nonlinear behavior of concrete in the finite element models was defined using the concrete damaged plasticity (CDP) model. In the study, the concrete damage plasticity (CDP) material model, which is included in the library of the preferred ABAQUS software for modeling concrete type materials, was preferred. CDP material model is a material model that allows the behavior of concrete under pressure and tension to be modeled separately, and the parameters of plasticization and damage under pressure and tension can be defined (Fig. 15).

Only the upper flange of the base of the support and the upper steel plate of the support were generated to model the support used in the experimental study. In the finite element model, the eight parts forming the support were defined using steel material and modeled using the C3D8R element. The parts were connected using the tie constraint. As a result, the support setup used in the experimental study was modeled appropriately in the finite element model. Rigid body constraint was applied to the support parts used in the model, and fixed support was defined at the reference points of the rigid bodies.

The impact hammer and the steel plate placed at the impact point on the RC slab were modeled using the C3D8R element. Rigid body constraint was applied to these two parts. Since the impact steel plate was tied to the RC plate using steel dowels in the experimental study, it was also tied using tie constraint in the finite element models. The hammer was placed close to the RC slab in the finite element model to shorten the analysis time. The vertical distance between the hammer's tip and the steel plate's upper surface placed on the RC slab was chosen as 1 mm. Accordingly, considering the velocity at the time of impact in the experimental study, a predefined velocity of 4.4 m/s was assigned to the hammer. In the finite element model, the hammer was allowed to move only in the vertical direction.

The contact between the surfaces of the parts in the finite element model was defined using the general contact interaction. Tangential and normal behavior were defined for the contact. A friction coefficient of 0.5 was defined in the contact interaction to consider the friction between different parts of the model. This friction coefficient value has also been used in studies found in the literature [20]. Since the test specimens were subjected to the impact of the hammer dropped under its weight, only the gravitational force was defined in the finite element model. A gravitational

acceleration of 9.81 m/s^2 was assigned to the model to simulate the real situation.

During modeling the RC slabs with steel fiber-reinforced concrete layers, three parts each 40 mm thick were modeled to consider the layers of the slab. The layers were connected using the tie constraint. Similar to the real situation, different concrete properties were assigned according to the locations of the layers used in each specimen. The steel plate used in the RC slabs was modeled using the C3D8R element. Studs welded to the steel plate tightly connect the steel plate to the RC slab. The tie constraint between the steel plate and the RC slab was defined at the anchor points.

To obtain reliable results in finite element analysis, the reliability of the results increases as the mesh size in the model decreases. However, the analysis time increases sharply as the mesh size decreases. Therefore, finding the optimum mesh size is a crucial step in the analysis. For this purpose, a convergence study examined different mesh sizes. The mesh sizes examined are 10 mm, 20 mm, 30 mm, and 40 mm. The maximum displacement values of Specimen-2 RC slab were compared for evaluation. The maximum displacement values of the Specimen-2 were calculated for 10 mm, 20 mm, 30 mm, and 40 mm mesh sizes, and relative dimensionless values were obtained by proportioning the displacement values to the displacement value of 10 mm mesh size. The relative dimensionless maximum displacements were 1.0, 1.066, 1.459, and 1.846, respectively. The difference between the maximum displacements in the case of 10 mm and 20 mm mesh sizes is negligible.

On the other hand, the analysis time for the 20 mm mesh size decreased by about 76% compared to the 10 mm mesh size. According to these results, the mesh size for the finite element analysis was 20 mm. The support, impact steel plate, and hammer mesh sizes were kept constant in the convergence study. The hammer and impact steel plate meshed with a 10 mm mesh size, and other parts in the models meshed with a 20 mm mesh size. During the analysis, the time increment of the models was automatically determined by the program, and the average time increment was determined as approximately 6.5×10^{-7} s. Figure 12 shows the meshed model of Specimen-1 RC slab as an example.

The maximum acceleration–time, maximum displacement–time, and impact loading–time histories obtained from the numerical analysis of the RC slabs included in the experimental program are compared with the experimental results and presented in Figs. 16, 17, and 18, respectively. A comparison of numerical and experimental maximum acceleration, minimum acceleration, maximum displacement, and

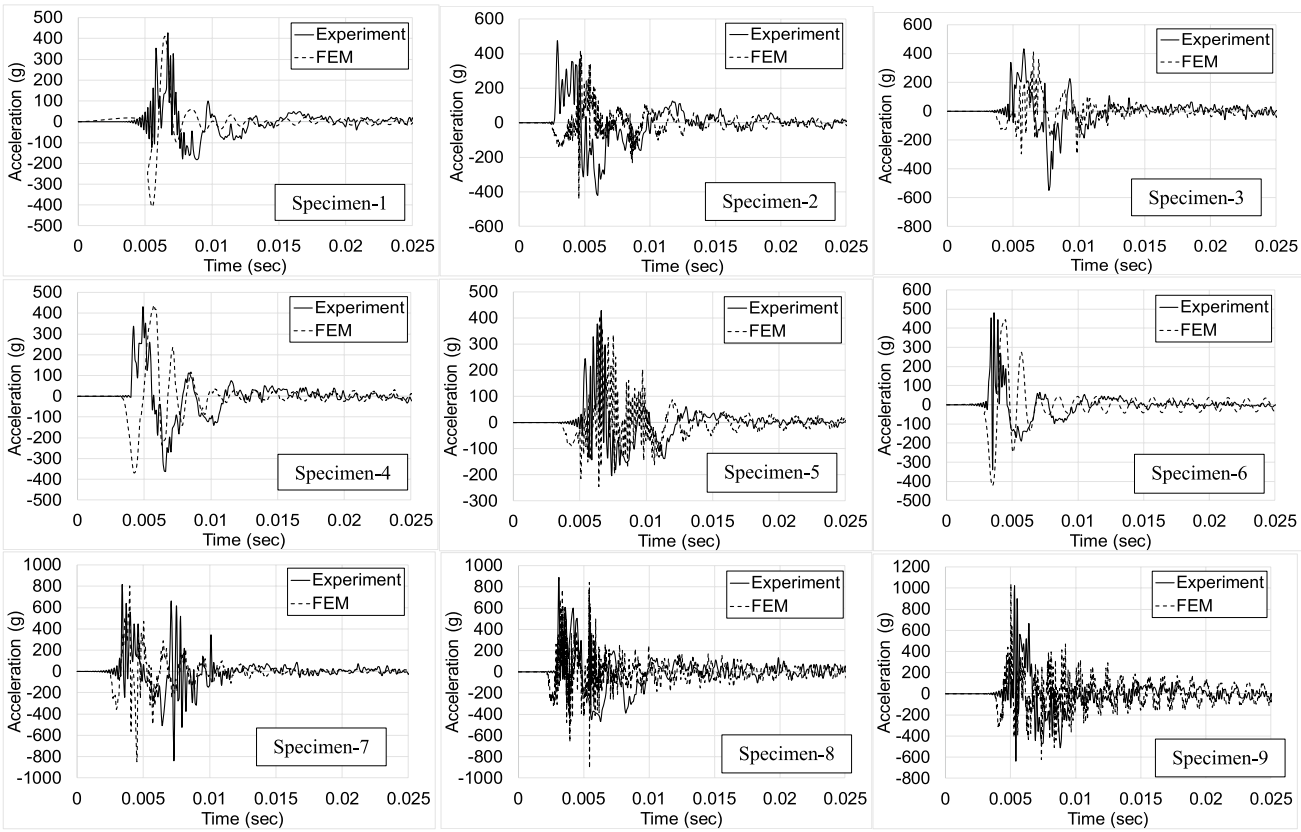

Fig. 16 Comparison of acceleration–time graphs obtained from experimental and finite element analysis

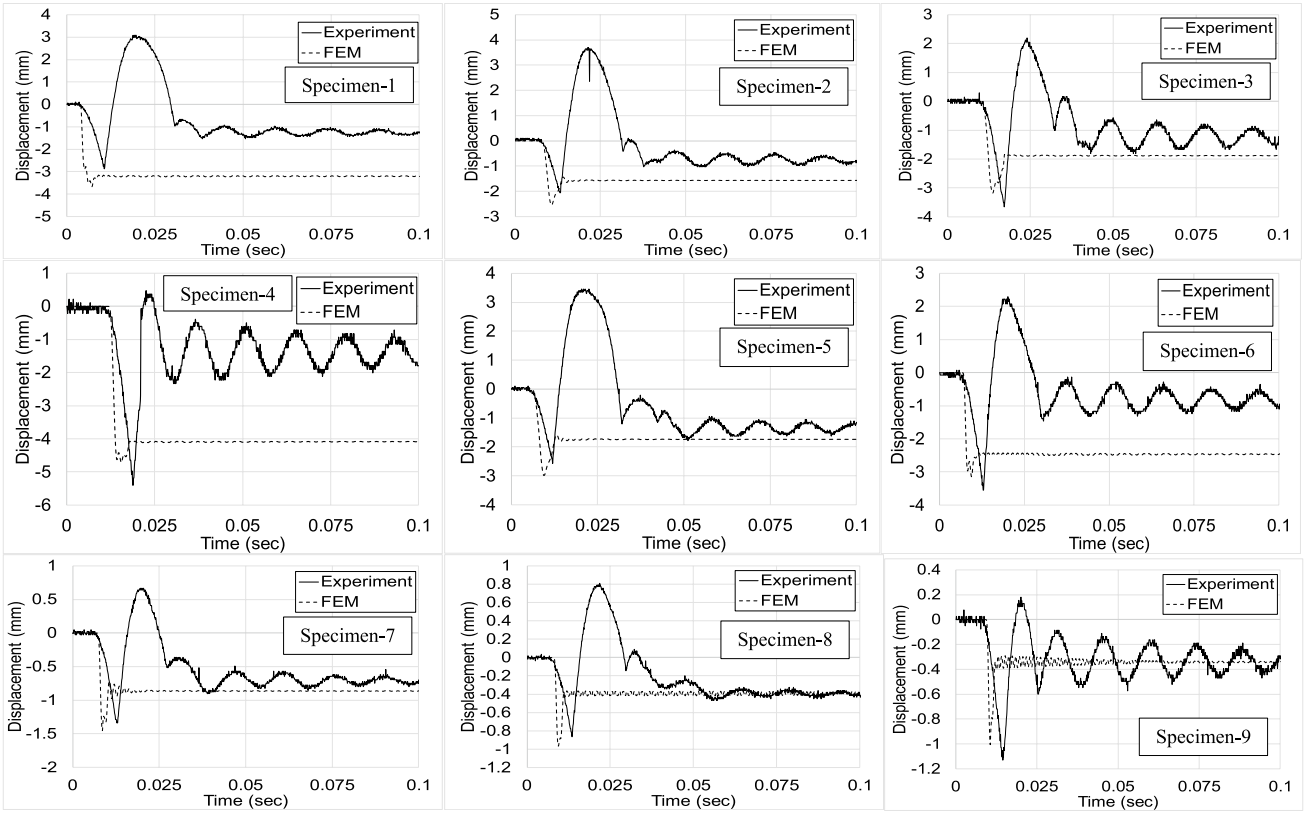

Fig. 17 Comparison of displacement–time graphs obtained from experimental and finite element analysis

residual displacement values of the RC slabs is presented in Table 6. When the maximum acceleration values calculated from the numerical analysis and the experimentally measured ones are compared, it can be seen that the results obtained from the finite element analysis of all RC slabs in the experimental series are in agreement with the experimental results and show very close values to each other. The ratios of the experimental maximum acceleration values to the ones obtained from the numerical analysis vary between 0.99 and 1.12. The average ratio of the experimental maximum acceleration values to the numerical results was 1.04. In addition to the fact that the maximum acceleration values are very close and compatible with each other when the numerical and experimental maximum acceleration–time distribution graphs presented in Fig. 16 are examined, it is seen that they show a consistent and similar behavior trend. Similarly, when the experimental and numerical impact load–time graphs given comparatively in Fig. 18 are compared, a good agreement is observed between the graphs. The ratios of the experimental maximum impact load values to the maximum impact loads obtained from the numerical analysis vary between 0.86 and 0.91, and the average ratio value is 0.89.

When Table 6, where the numerical analysis values are presented, is examined, it is seen that the difference between the numerically calculated maximum displacement values and the experimental results is quite big. The numerical maximum displacement values of all the experimental elements in the experimental program showed smaller values than the experimentally measured maximum values. The ratios of the experimental maximum displacement values to those calculated numerically vary between 1.24 and 2.26. The fact that the numerical maximum displacement values are much lower than the experimental values is an important indicator that the models behave more rigidly than the real specimens. Moreover, when the experimental and numerical displacement graphs presented comparatively in Fig. 17 are examined, it is observed that the vibration after the collision is damped more quickly in the numerical graphs. However, after the maximum displacement value is reached, the amplitude of the damping phase of the graphs is higher in the experimental graphs compared to the numerical graphs. This behavior trend can be seen in all displacement graphs similarly. This situation led to the thought that the experimental specimens showed more ductile behavior than the numerical models [3]. When the residual displacement values calculated as a result of the numerical analysis are compared with the experimental results, it is observed that most of them are higher than the experimental results. The ratios of the experimentally measured residual displacement

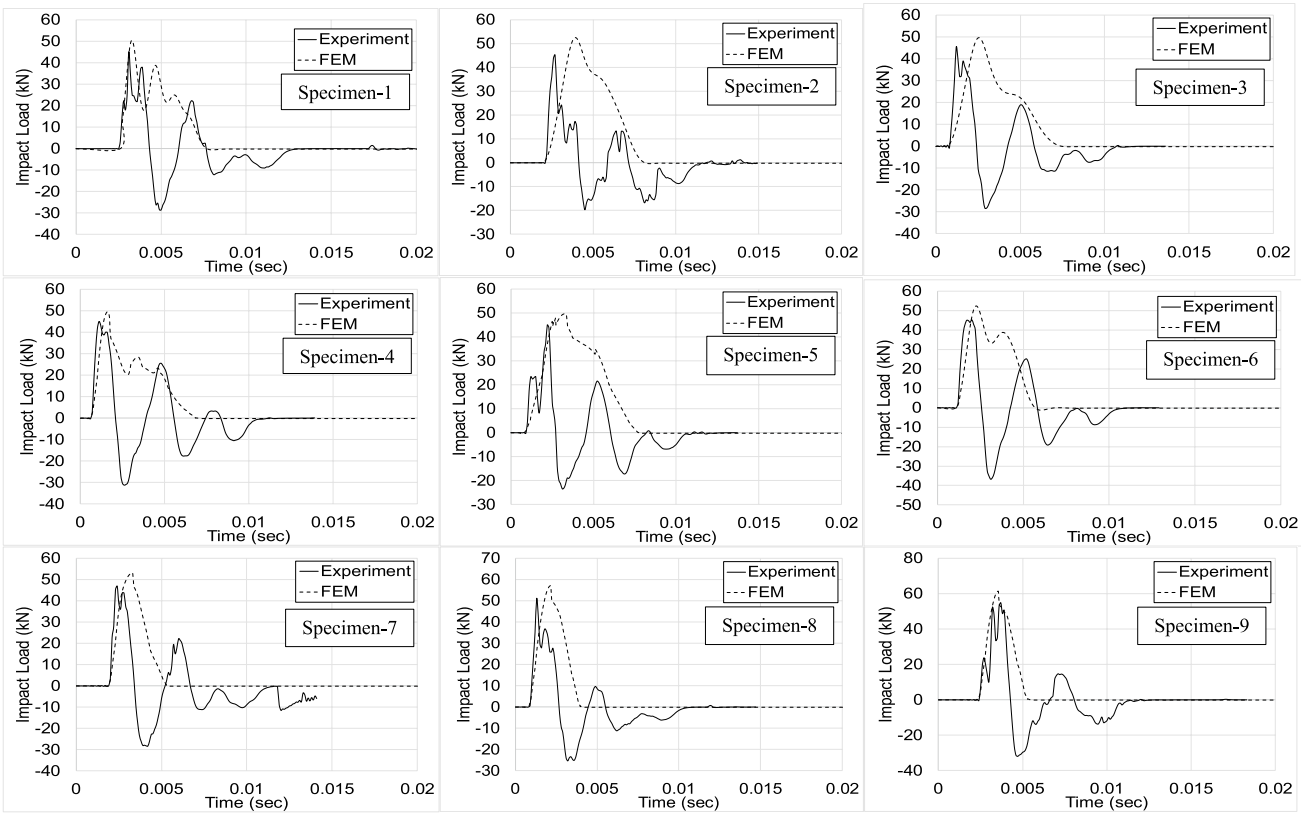

Fig. 18 Comparison of impact load–time graphs obtained from experimental and finite element analysis

Table 6 Comparison of experimental and numerical results

Specimen #	Acceleration (g)					Maximum displacement (mm)			Residual displacement (mm)		
	Experimental		ABAQUS		Ratio[a]	Experimental	ABAQUS	Ratio[b]	Experimental	ABAQUS	Ratio[c]
	Max	Min	Max	Min							
1	427.33	−181.99	410.4	−409.08	1.04	5.97	3.66	1.63	1.29	3.18	0.41
2	472.46	−418.76	420.79	−440.12	1.12	5.76	2.55	2.26	0.77	1.57	0.49
3	433.64	−547.10	412.66	−296.92	1.05	5.84	3.18	1.84	1.29	1.88	0.69
4	431.46	−361.28	436.96	−369.53	0.99	5.87	4.72	1.24	1.31	4.08	0.32
5	425.41	−203.66	409.15	−244.83	1.04	6.03	2.99	2.02	1.31	1.74	0.75
6	470.12	−339.48	444.95	−422.81	1.06	5.85	3.14	1.86	0.80	2.46	0.33
7	816.85	−839.53	803.94	−848.17	1.02	2.01	1.45	1.39	0.72	0.87	0.83
8	889.27	−467.00	842.48	−909.56	1.06	1.67	0.97	1.72	0.41	0.38	1.08
9	1022.59	−637.75	1038.89	−622.88	0.98	1.31	1.01	1.3	0.32	0.34	0.94

[a]Ratio of experimental maximum acceleration values to ABAQUS FEM results

[b]Ratio of experimental maximum displacement values to ABAQUS FEM results

[c]Ratio of experimental residual displacement values to ABAQUS FEM results

values to the numerically calculated results are observed to vary between 0.32 and 1.08.

It is thought that the differences between the numerical and experimental results, especially the maximum and residual displacement values, are due to the heterogeneity and anisotropy of concrete and the differences between the experimental support and the finite element model support conditions. Material models in finite element software consider concrete completely homogeneous and isotropic, and it is impossible to consider the heterogeneity and anisotropy

of concrete in the modeling. In addition, the homogeneity of concrete is affected by some factors such as environmental conditions, curing conditions, compaction, and maintenance [7]. Moreover, the support condition used in the finite element modeling may not exactly resemble those applied in the experiments. The support conditions defined in the finite element models provides exact restraint. However, in reality, there may be some differences in the support condition that is tried to be provided experimentally [21].

In addition, ABAQUS finite element software cannot automatically identify the effect of strain rate on material properties. To consider the strain rate effect in ABAQUS software, as detailed in the numerical analysis section, the user enlarged material model values by multiplying them by a dynamic increase factor and entered them into the software. However, this method may not exactly reflect the effect of strain rate on concrete behavior [21]. In addition, determining the appropriate strain rate increase factor for RC members under impact loading is a complex problem. There are even fewer studies in the literature on the dynamic increase factor of RC elements produced using fiber-reinforced concrete subjected to impact loading. The problems mentioned above encountered during the modeling of RC elements subjected to impact loading have been similarly expressed in many studies in the literature [22].

Another result from the numerical analysis of the RC slabs included in the experimental program is the crack and damage distributions caused by the applied impact load. For this purpose, the DAMAGET function was used. This function shows the tensile damage distribution in the RC slabs. DAMAGET function distributions of the specimens obtained from the numerical analysis are given in Fig. 19. When the crack distributions obtained from the experimental study and the DAMAGET function distributions obtained from the numerical analysis are compared, it is observed that there is a consistency between them. The cracks obtained from the numerical analysis are mainly concentrated on the tensile surface of the RC slabs in the central region, where the impact load was applied, and show diagonal progression toward the supports. In addition, when the DAMAGET function distributions obtained from the numerical analysis are examined, it is observed that the RC slabs with a steel

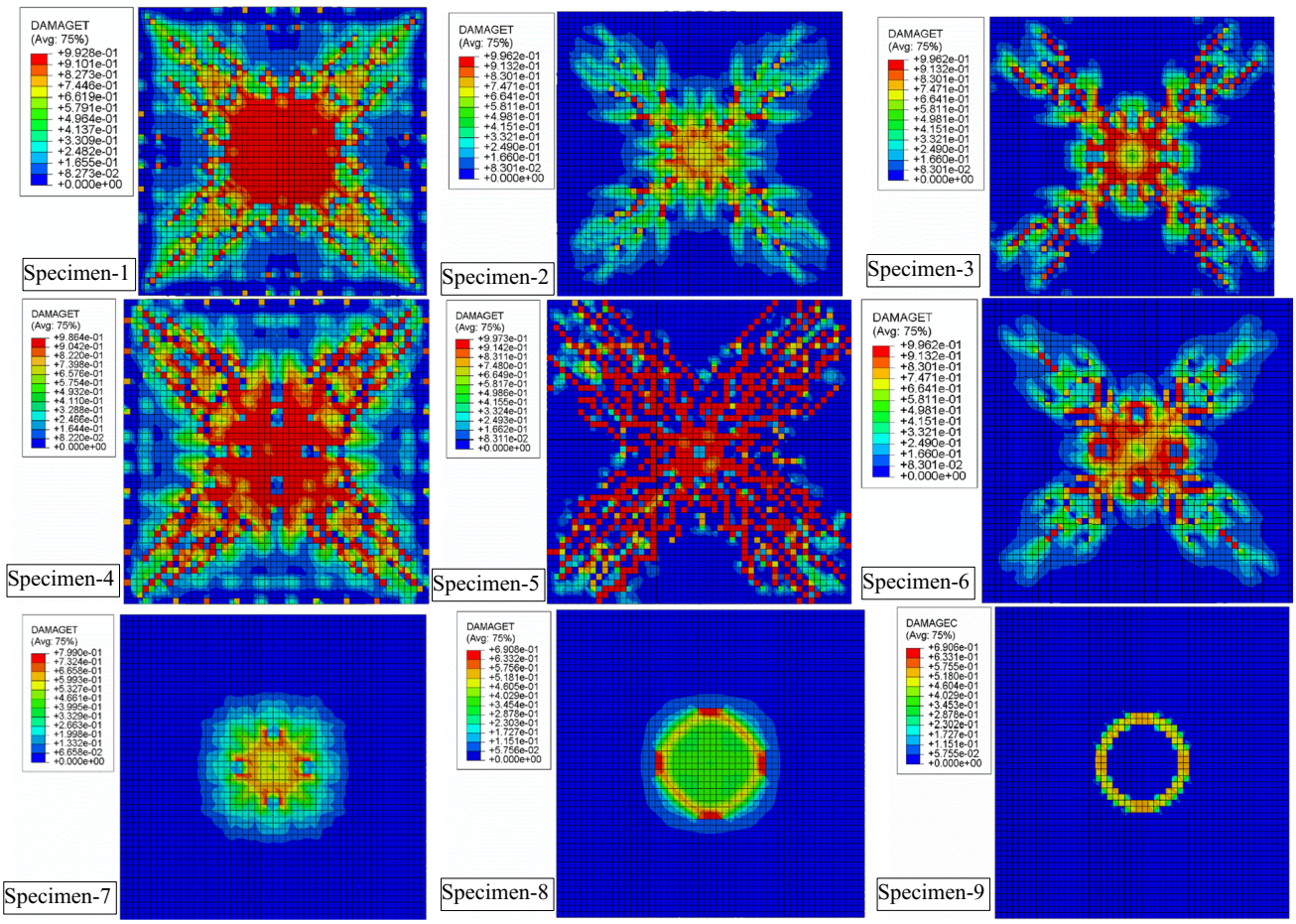

Fig. 19 Damage distributions obtained as a result of finite element analysis (DAMAGET)

fiber-reinforced concrete layer on their tensile surface are less damaged compared to the reference Specimen-1. The level of damage remained at a much more limited level in the specimens with a steel plate layer on the tensile surface. These findings are consistent with the results found in the experimental study.

5 Conclusion

Within the scope of this study, it is aimed to investigate the effectiveness of strengthening techniques by adding a steel fiber-reinforced concrete layer and a steel plate layer to improve the behavior of RC slabs, which have a high potential to be subjected to impact loading in RC structures, and to increase their performance under impact loading. It is known that RC structural elements designed without considering the effects of impact loading in their designs can suffer severe damage and even collapse completely under the effect of such loads. For this reason, it is aimed to determine an easy-to-apply, low-cost strengthening method that does not need special workmanship and complex application details to improve the performance and behavior of RC slabs under the effect of impact loading. An experimental study was planned to investigate the effects of two different techniques selected for this purpose: applications of steel fiber-reinforced concrete layer and steel layer, on the behavior of RC slabs under impact loading. In addition, numerical analyses of the RC slabs tested within the scope of the experimental study were performed with ABAQUS finite element software and compared with experimental results. With this comparison made between the experimental and numerical analysis results, comments were made about the extent to which the numerical analysis models were consistent with the experimental results and gave successful results. The conclusions obtained from the study are listed below.

- When the test results of the RC slabs included in the experimental program were compared, the use of steel fiber-reinforced concrete layer and steel plate layer positively affected and improved the impact performance. The use of steel fiber-reinforced concrete increased the maximum acceleration values of the RC slabs and decreased the maximum and residual displacement values. The maximum acceleration values of the specimens produced using SFRC layer were obtained on average 4.5% higher than the reference Specimen-1. The maximum displacement and plastic residual displacement values of the reference Specimen-1 were calculated to be 1.7% and 25.1% higher than the SFRC specimens, respectively. Adding steel fiber to concrete increased concrete's compressive strength, tensile strength, toughness, and energy absorption capacity. In addition, steel fiber delayed the formation and propagation of cracks. Using steel fiber reduced the damage formed in the RC slab by reducing the width of cracks and imparting multiple cracking behaviors to the slab.
- Compressive stress occurs on the upper surface of the RC slabs, where impact loading is applied, and tensile stress occurs on the lower surfaces. Due to the bending deformation and vertical displacements that occurred due to impact loading on the slabs, compression stresses occurred on the upper surface of the slabs and tensile stresses occurred on the lower surface. To increase the performance of the specimens under impact loading, steel plates and fiber-reinforced concrete layers placed on the lower tensile surface increased the tensile capacity in this region. Steel plate and fiber-reinforced concrete layers placed on the upper surfaces of the slabs increased the compressive strength in this area and increased their performance under impact loading.
- It was shown that the combined use of steel fiber and steel plate layer significantly improved the impact performance of RC slabs. Using the steel plate layer in the RC plate significantly increased the maximum acceleration values and remarkably reduced the maximum and residual displacements. The maximum acceleration values of the specimens using steel plates were calculated to be 112.8% higher on average than the reference Specimen-1. The maximum displacement and plastic residual displacement values of the reference Specimen-1 are on average 270% and 199% larger, respectively, than the specimens using steel plates. It was shown that the combined use of steel fiber and steel plate layer significantly increased the rigidity, toughness, strength, and, consequently, the RC slab's impact performance. The damage that occurred in the RC slab under the applied impact energy remained at a very limited level.
- It was observed that the improvement in the impact performance of the RC slab was much greater when the steel plate layer was used on the tension side of the RC slab. The maximum acceleration value of Specimen-8 was 8.9% higher, and the maximum displacement value was 16.9% less than that of Specimen-7. A reduction of 43.1% was observed in the residual displacement value, which was also reflected in the reduction in the number and width of cracks.
- Using the steel plate layer on both surfaces of the RC slab increased the impact performance even more than using it on only one side. Specimen-9 has 25.2% and 15% higher maximum acceleration, 34.8% and 21.6% lower maximum displacement, and 55.6% and 22% lower residual displacement than Specimen-7 and Specimen-8, respectively. As a result of the higher impact strength of Specimen-9, the level of damage was significantly reduced.

- When the impact performances of the RC slabs were compared, it was observed that the RC slabs without steel plate, in which the position of the steel fiber-reinforced concrete layer was changed, showed similar performances. Specimen-4 and Specimen-6 showed the highest impact performance among the RC slabs with steel fiber-reinforced concrete layers on different positions. Among the RC slabs in the experimental program, the best impact performance was shown by Specimen-9, which had a steel plate layer on both sides and steel fiber.
- The maximum acceleration values and the general behavior trends of the acceleration–time histories obtained from the numerical analyses performed within the scope of the study using ABAQUS finite element software are quite consistent with the experimental results, and the values are close to each other. However, it has been observed that there are quite big differences between the maximum and residual displacement values calculated from the numerical analysis and the results obtained from the experimental study. The displacement values calculated from the numerical analyses were obtained smaller than the experimental values, and the numerical analysis models exhibited a much more rigid behavior than the experimental elements.

Funding Open access funding provided by the Scientific and Technological Research Council of Türkiye (TÜBİTAK).

Data availability No new data that requires sharing has been produced within the scope of this article.

Declarations

Conflict of interest All of the authors declare that he/she has no conflict of interest.

References

1. Anıl Ö, Kantar E, Yılmaz MC. Low velocity impact behavior of RC slabs with different support types. Constr Build Mater. 2015;93:1078–88.
2. Yılmaz T, Anıl Ö, Tuğrul Erdem R. Experimental and numerical investigation of impact behavior of RC slab with different opening size and layout. Structures. 2022;35:818–32.
3. Yılmaz T, Kıraç N, Anıl Ö, Erdem RT, Kaçaran G. Experimental investigation of impact behaviour of RC slab with different reinforcement ratios. KSCE J Civ Eng. 2020;24(1):241–54.
4. Shakir QM, Abdlsaheb SD. Rehabilitation of partially damaged high strength RC corbels by EB FRP composites and NSM steel bars. Structures. 2022;38:652–71.
5. Shakir QM, Abdlsaheb SD. Strengthening of the self-compacted reinforced concrete corbels using NSM steel bars and CFRP sheets techniques. J Eng Sci Technol. 2022;17(3):1764–80.
6. Yılmaz T, Kıraç N, Anıl Ö, Erdem RT, Sezer C. Low-velocity impact behaviour of two way RC slab strengthening with CFRP strips. Constr Build Mater. 2018;186:1046–63.
7. Şengel HS, Erol H, Yılmaz T, Anıl Ö, Can Gürdal H, Muhammed Uludoğan A. Low-velocity impact behavior of two-way RC slab strengthening with carbon TRM strips. Structures. 2022;44:1695–714.
8. Banyhussan QS, Yıldırım G, Anıl Ö, Erdem RT, Ashour A, Şahmaran M. Impact resistance of deflection-hardening fiber reinforced concretes with different mixture parameters. Struct Concr. 2019;20(3):1036–50.
9. Zhao W, Guo Q. Experimental study on impact and post-impact behavior of steel-concrete composite panels. Thin Walled Struct. 2018;130:405–13.
10. Shakir QM, Hanoon HK. New models for reinforced concrete precast hybrid deep beams under static loads with curved hybridization. Structures. 2023;54:1007–25.
11. Shakir QM, Hanoon HK. Behavior of high-performance reinforced arched-hybrid self-compacting concrete deep beams. J Eng Sci Technol. 2023;18(1):792–813.
12. Othman H, Marzouk H. An experimental investigation on the effect of steel reinforcement on impact response of reinforced concrete plates. Int J Impact Eng. 2016;88:12–21. https://doi.org/10.1016/j.ijimpeng.2015.08.015.
13. Yuan J, Wu J, Su T, Dadi Lin D. Dynamic response of reinforced recycled aggregate concrete pavement under impact loading. Appl Sci. 2022;12:8804. https://doi.org/10.3390/app12178804.
14. Yılmaz T, Kıraç N, Anıl Ö. Experimental investigation of axially loaded reinforced concrete square column subjected to lateral low-velocity impact loading. Struct Concr. 2019;20(4):1358–78.
15. Lu J, Wang Y, Zhai X. Response of flat steel-concrete-corrugated steel sandwich panel under drop-weight impact load by a hemispherical head. J Build Eng. 2021;44(May): 102890.
16. Hrynyk TD, Vecchio FJ. behavior of steel fiber-reinforced concrete slabs under impact load. ACI Struct J. 2014;111(5):1.
17. Simulia. ABAQUS 6.14 user's manuals, Dassault Systèmes Simulia Corp.; 2016.
18. Senthil K, Kubba Z, Sharma R, Thakur A. Experimental and numerical investigation on reinforced concrete slab under low velocity impact loading. IOP Conf Ser Mater Sci Eng. 2021;1090(1):012090.
19. Anas SM, Alam M, Shariq M. behavior of two-way RC slab with different reinforcement orientation layouts of tension steel under drop load impact. Mater Today Proc. 2022;2022:1.
20. Li C, Hao H, Bi K. Numerical study on the seismic performance of precast segmental concrete columns under cyclic loading. Eng Struct. 2017;148:373–86.
21. Yılmaz MC, Mercimek Ö, Ghoroubi R, Anıl Ö, Gültop T. Investigation of support type effect on plastic hinges in RC beam under impact load. Struct Concr. 2021;22(4):2049–69.

22. Demirhan S, Yıldırım G, Banyhussan QS, Koca K, Anıl Ö, Erdem RT, Şahmaran M. Impact behaviour of nano-modified deflection-hardening fibre reinforced concretes. Mag Concr Res. 2019;2019:1–23.